POLITECNICO DI MILANO





Automatic Control

Motion control

Standard control techniques

Prof. Luca Bascetta (luca.bascetta@polimi.it)

Politecnico di Milano

Dipartimento di Elettronica, Informazione e Bioingegneria

Motivations

A servomechanism (or servo) is composed of

- a motor
- a transmission chain
- a load
- one or more position sensors
- a control board, including a power stage

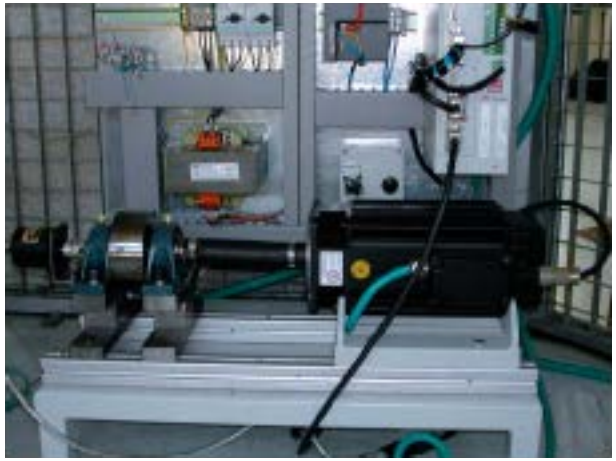

We will now introduce the characteristics of a motion control problem, i.e., how to control the position of the load regulating motor torque.

We will consider different scenarios, in terms of:

- number of available position sensors
- location of each position sensor (motor side or load side)
- mechanical characteristics of the transmission chain (rigid or elastic)

Modelling a rigid servomechanism (I)

We start introducing the model of a servomechanism with rigid transmission chain.

First, consider the model of a DC motor.

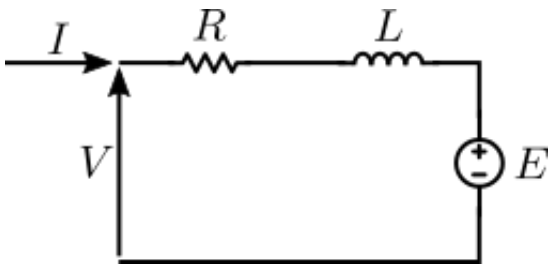

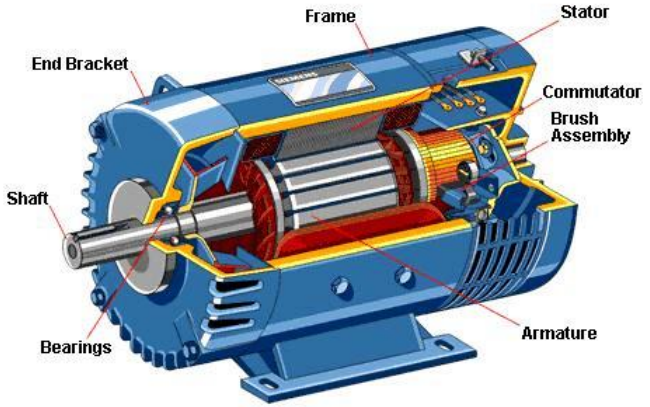

The voltage applied to armature windings generates a current that depends on the motor characteristics (RL equivalent circuit) and the back-EMF voltage.

It can be shown that the motor generates a torque proportional to the armature current.

In classical DC motors, current commutation is operated by the commutator and by brushes.

In robots and machine tools, brushless motors are usually adopted.

Modelling a rigid servomechanism (II)

A DC motor is described by the following equations

$$V(t) = RI(t) + L\frac{\mathrm{d}I(t)}{\mathrm{d}t} + E(t)$$

$$E(t) = K\omega_m(t)$$

$$\tau(t) = KI(t)$$

$$\tau(t) = J_m\dot{\omega}_m(t)$$

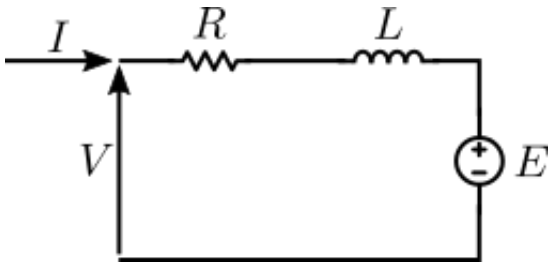

or, equivalently, by the following block diagram

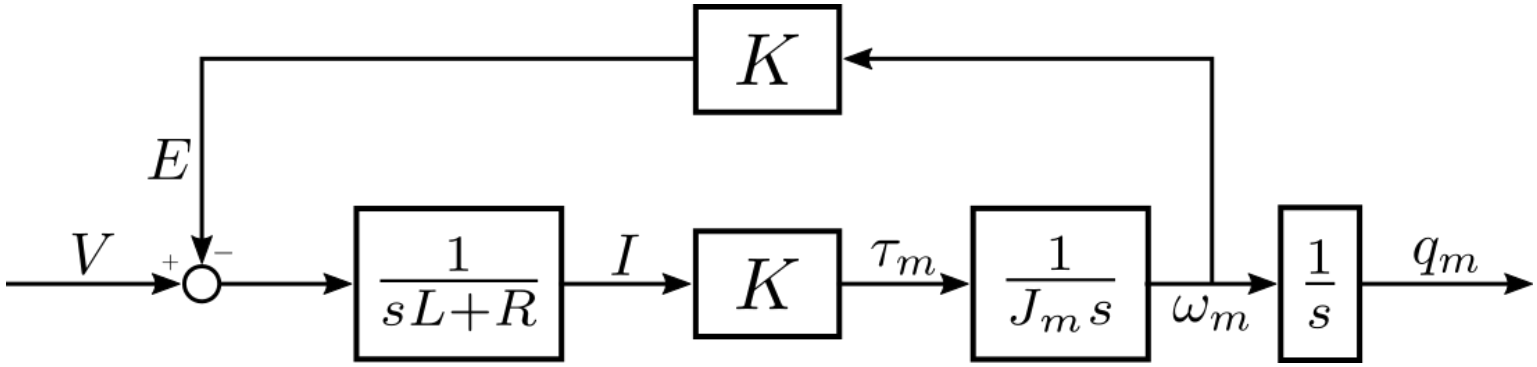

Modelling a rigid servomechanism (III)

If we assume that the transmission chain is rigid, the subsystem composed by the motor, the transmission chain and the load is described by the following equations

$$J_m \ddot{q}_m + D_m \dot{q}_m = \tau_m - \tau_{ms} \qquad \text{motor}$$

$$J_l \ddot{q}_l = n\tau_{ms} - \tau_l \qquad \text{load}$$

$$q_m = n q_l \qquad \text{transmission chain}$$

that can be merged obtaining

$$\left(J_m + J_{lr}\right) \ddot{q}_m + D_m \dot{q}_m = \tau_m - \tau_{lr}$$

where

$$J_{lr} = \frac{J_l}{n^2} \qquad \tau_{lr} = \frac{\tau_l}{n}$$

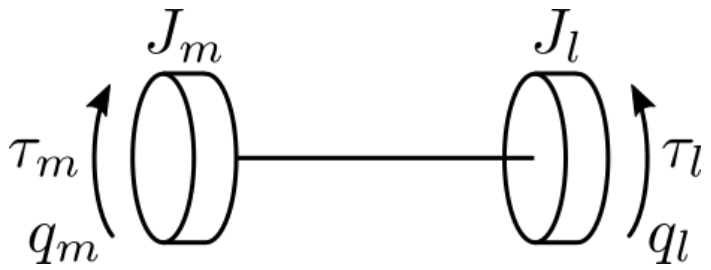

Modelling a rigid servomechanism (IV)

The model is represented by the following block diagram

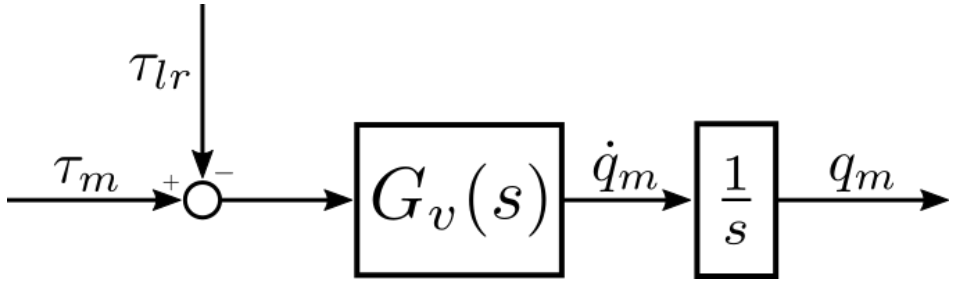

where

$$G_v(s) = \frac{1}{D_m + s\left(J_m + J_{lr}\right)}$$

If friction D_m is negligible, the model simplifies as

$$G_v(s) = \frac{1}{J_m + J_{lr}} \frac{1}{s}$$

Modelling a rigid servomechanism (V)

Combining the two models, we obtain the following block diagram

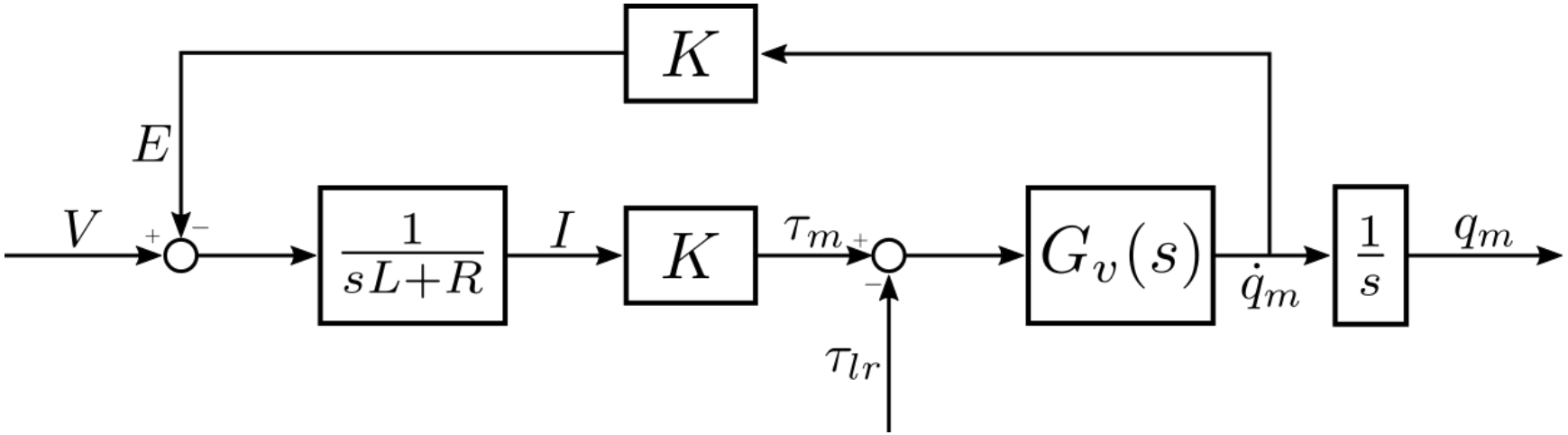

Control system architecture (I)

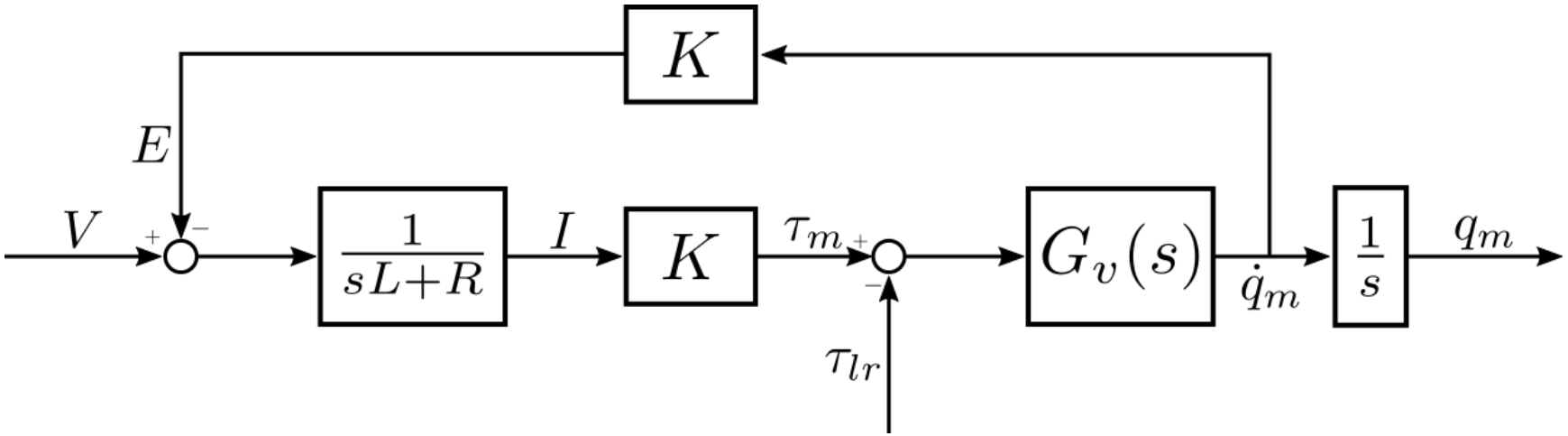

Taking into account the structure of the model, we can simplify the design of the control system using a cascaded control architecture.

We can identify three intermediate variables:

- motor current
- motor velocity
- motor position

that give rise to three loops.

Control system architecture (II)

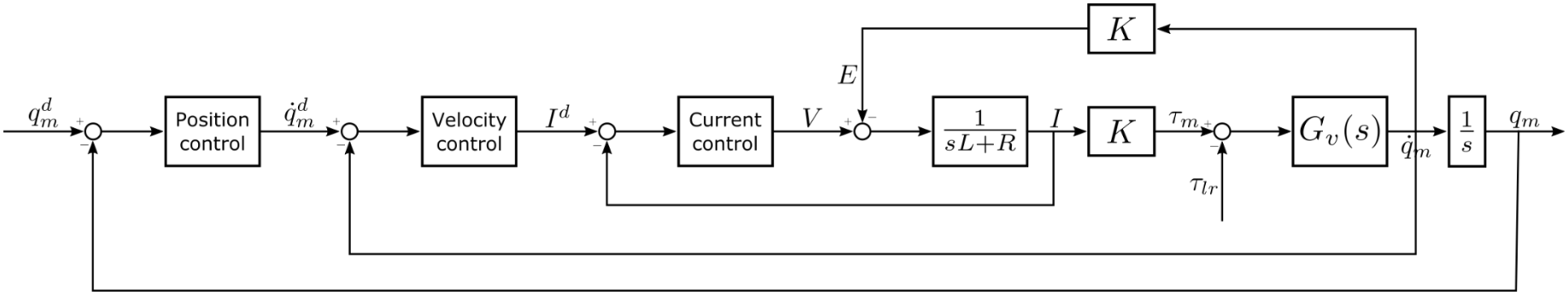

The cascaded control architecture is composed of:

- a PI current controller
- a PI velocity controller
- a P position controller

As in any cascaded control architecture the tuning of the control system is performed starting from the inner loop.

We will now consider the design of each loop, under the assumption of rigid transmission.

Current control

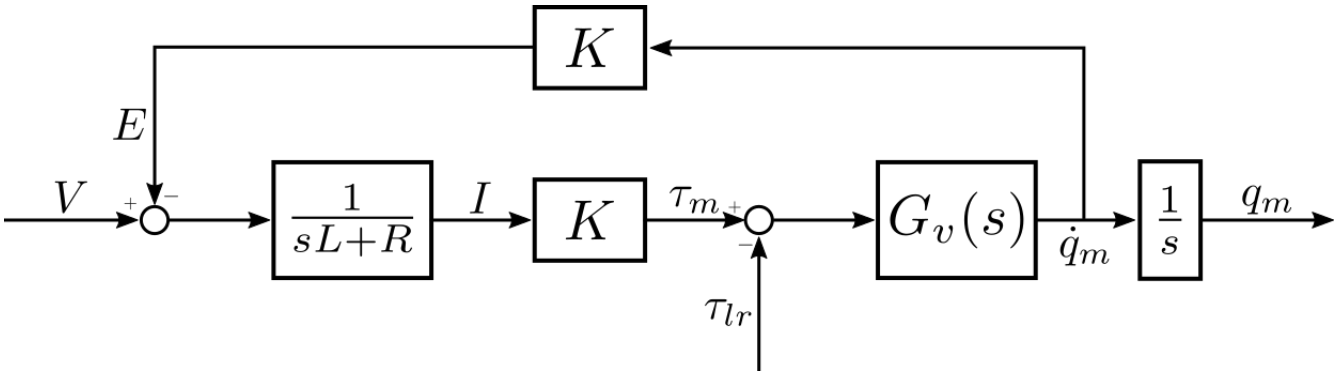

The design of the current controller is based only on the electrical dynamics.

Considering that these dynamics are usually very fast, an high bandwidth loop can be designed (thousand of rad/s).

Back-EMF acts on the loop as a slow load disturbance, as it depends on the mechanical dynamics, and is thus rejected by the closed-loop system.

Thanks to the frequency separation between the electrical and mechanical dynamics, the velocity regulator assumes that there is an algebraic relation between the desired and actual current

$$\tau_m(t) = KI(t) \approx KI^d(t)$$

Velocity control (I)

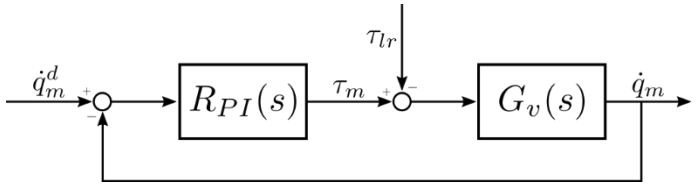

Velocity control is accomplished using a PI controller

$$R_{PI}(s) = K_{P_v}\left(1 + \frac{1}{sT_{I_v}}\right) = K_{P_v}\frac{1 + sT_{Iv}}{sT_{Iv}}$$

The loop transfer function is given by

$$L_v(s) = R_{PI}(s)G_v(s) = \frac{K_{P_v}\mu}{s}\frac{1 + sT_{Iv}}{sT_{Iv}}$$

If a large value for T_{Iv} is selected, so that a low frequency zero is generated, the loop transfer function is approximated, around the crossover frequency, by its high-frequency approximation

$$L_v(s) \approx \frac{\omega_{c_v}}{s} \quad \Rightarrow \quad \omega_{c_v} = K_{P_v}\mu$$

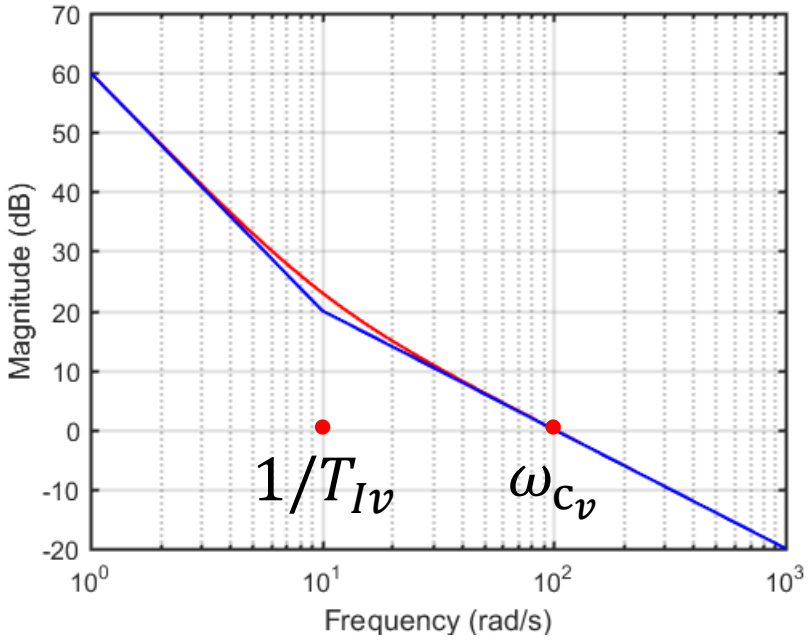

Velocity control (II)

Summarizing, we will select the PI parameters following the rules

$$K_{P_v} = \frac{\omega_{c_v}}{\mu}$$

$$\frac{1}{T_{I_v}} = (0.1 \div 0.3)\,\omega_{c_v}$$

Position control

The velocity loop is seen by the position loop as a first order low-pass filter.

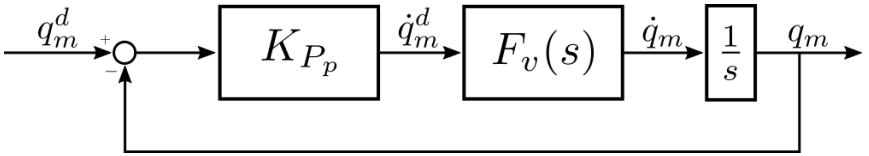

The plant transfer function used to tune the position controller is thus

$$F_v(s)\frac{1}{s} \approx \frac{1}{1+s/\omega_{c_v}}\frac{1}{s}$$

and the loop transfer function

$$L_p(s) = K_{P_p}F_v(s)\frac{1}{s} = \frac{K_{P_p}}{s\left(1+s/\omega_{c_v}\right)}$$

Selecting $K_{P_p} \ll \omega_{c_v}$ we have

$$\omega_{c_p} \approx K_{P_p}$$

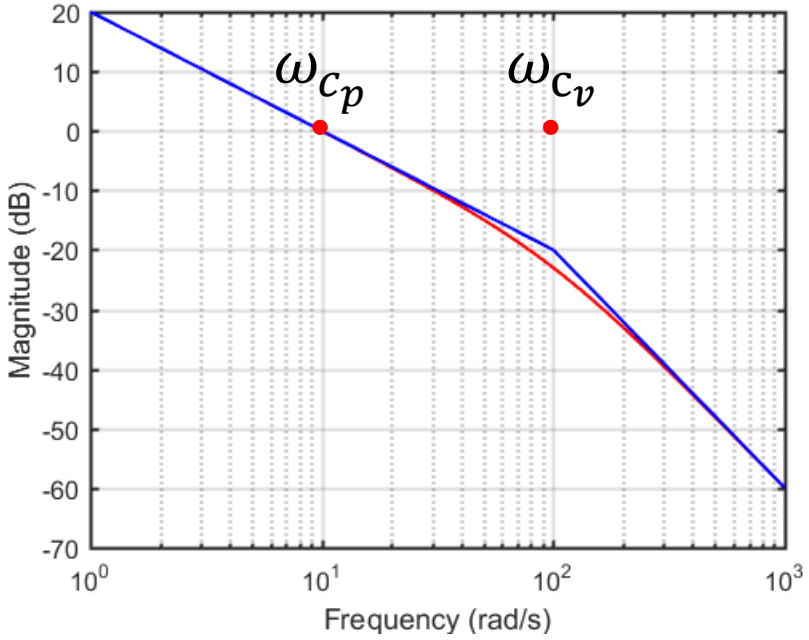

Velocity feedforward (I)

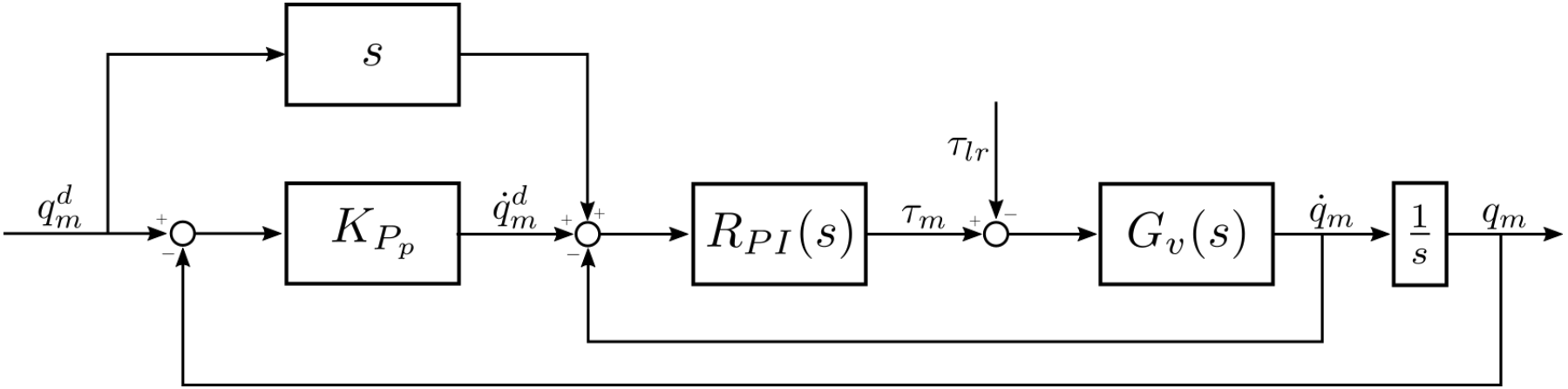

In order to increase the performance of the system, we can introduce a velocity feedforward action.

Sometimes a weighted feedforward action is used ($k_{ff} \in [0,1]$)

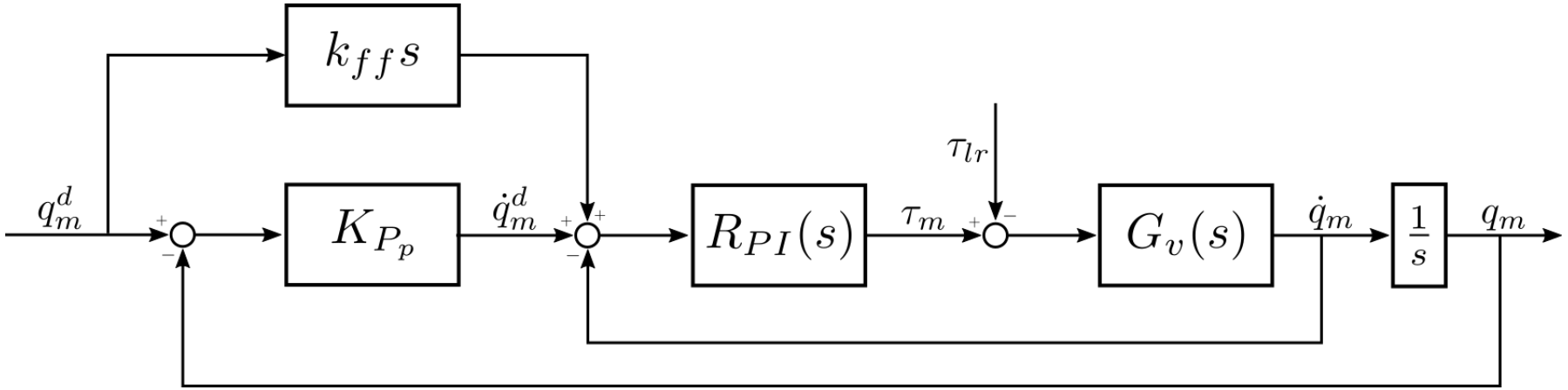

Velocity feedforward (II)

If a unitary feedforward is considered, and the velocity measurement is substituted by the derivative of the position measurement, it can be easily shown that the P/PI scheme is equivalent to a PID regulator.

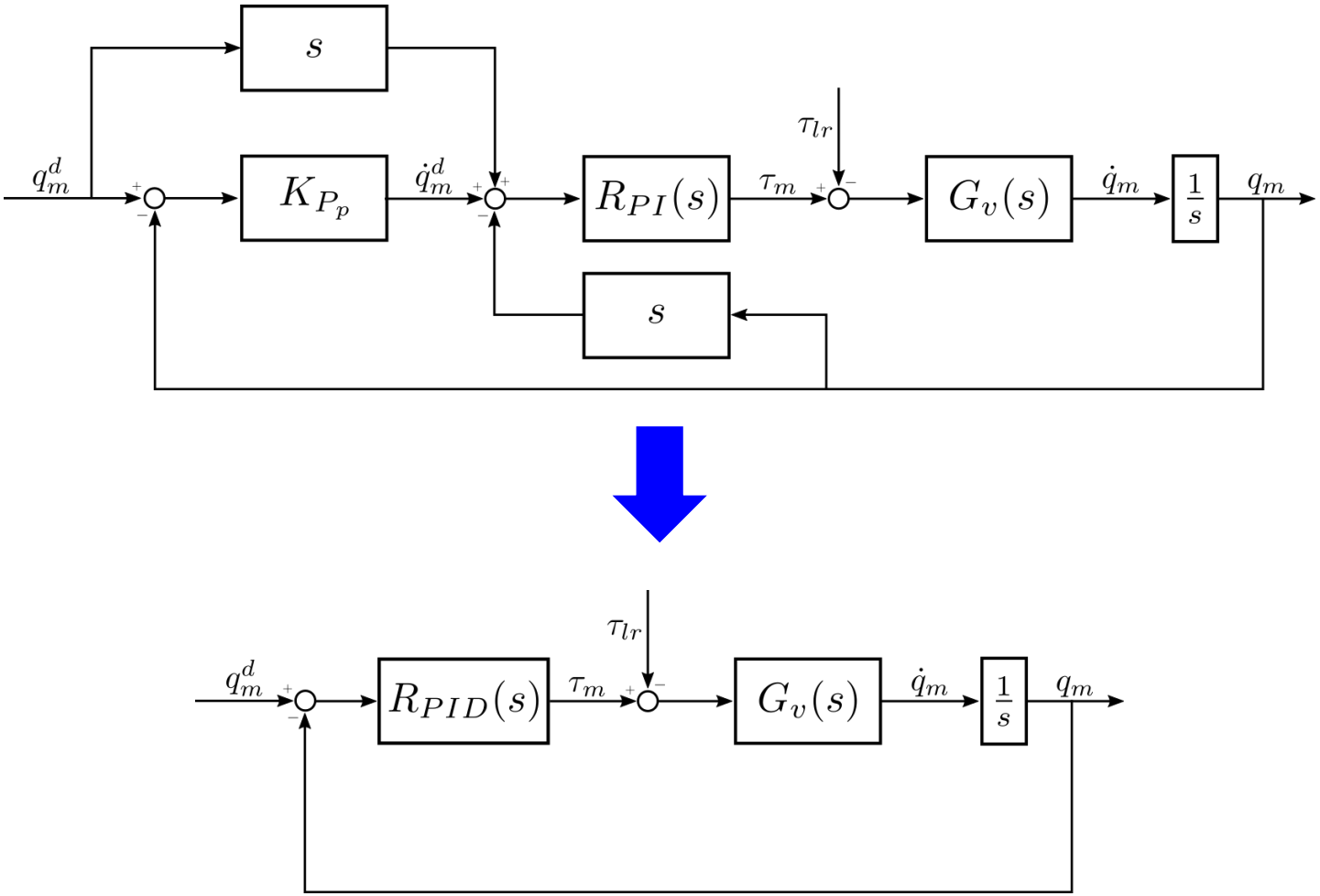

Velocity feedforward (III)

We can easily show the equivalence.

Let's compute the transfer function of the control system

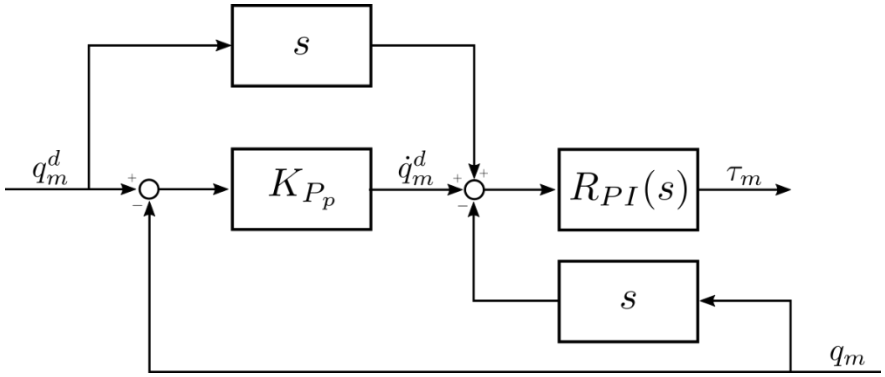

$$\tau_m(s) = R_{PI}(s)\left(sq_m^d(s) - sq_m(s) + K_{P_p}\left(q_m^d(s) - q_m(s)\right)\right)$$

$$= K_{P_v}\left(1 + \frac{1}{sT_{I_v}}\right)\left(s + K_{P_p}\right)\left(q_m^d(s) - q_m(s)\right)$$

$$= R_{PID}(s)\left(q_m^d(s) - q_m(s)\right)$$

and

$$R_{PID}(s) = K_P\left(1 + \frac{1}{sT_I} + sT_D\right)$$

$$K_P = K_{P_v}\left(K_{P_p} + \frac{1}{T_{I_v}}\right) \qquad T_D = \frac{K_{P_v}}{K_P} \qquad T_I = \frac{K_P T_{I_v}}{K_{P_p} K_{P_v}}$$

Limitations of the rigid servo model

The design based on the rigid model of the servomechanism does not reveal any limitation to the crossover frequency, i.e., it seems that the bandwidth of the system can be arbitrarily increased.

In a real system, however, as the bandwidth increases undesired vibrations, noise and torque saturation appear.

We conclude that the rigid model is too simple and it is not able to represent all the control relevant dynamics.

We will now study a more complex model of the servomechanism that is able to correctly interpret what happens to a real system when the bandwidth increases.

Two-mass model of a servomechanism (I)

To overcome the limitations of the rigid model, let's assume that the motor is connected to the load through an elastic transmission.
The model than becomes

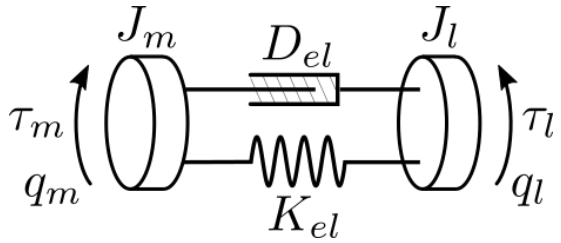

$$J_m\ddot{q}_m + D_m\dot{q}_m = \tau_m - \tau_{ms} \qquad \text{motor model}$$

$$J_l\ddot{q}_l = n\tau_{ms} - \tau_l \qquad \text{load mode}$$

$$\tau_{ms} = K_{el}\left(q_m - nq_l\right) + D_{el}\left(\dot{q}_m - n\dot{q}_l\right) \qquad \text{transmission model}$$

and the corresponding block diagram is

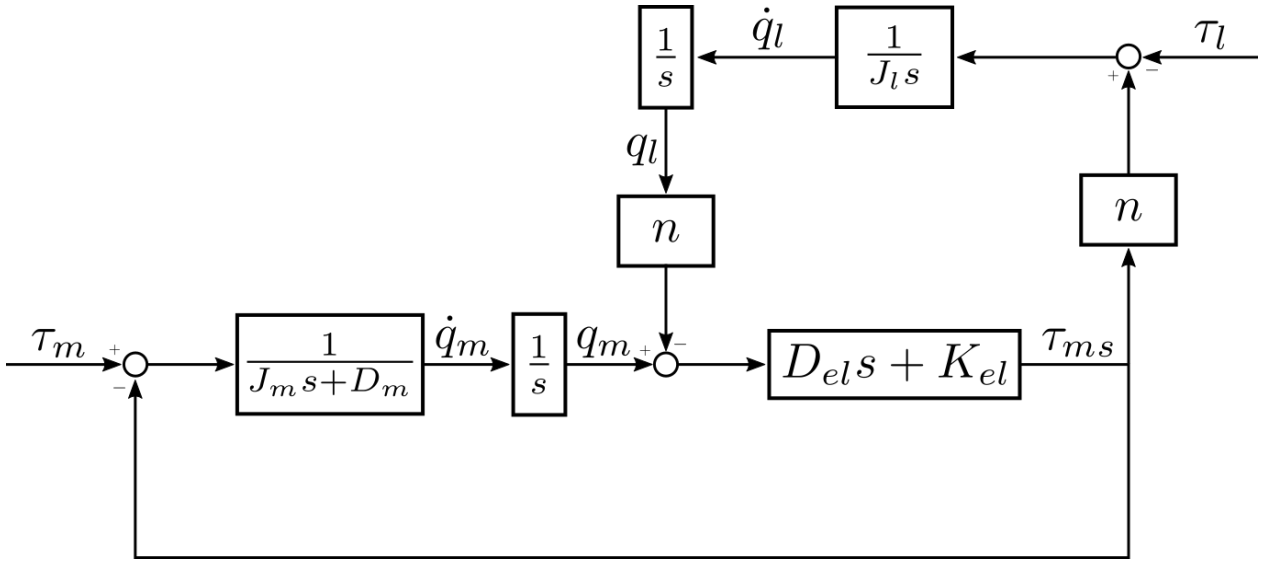

Two-mass model of a servomechanism (II)

Let's consider the response of the system to a variation of motor torque, neglecting load torque.

We can consider either the transfer function from motor torque to motor position or to load position.

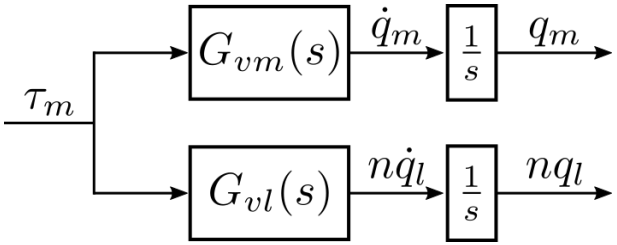

The system can be thus interpreted as a SITO (Single Input Two Outputs) dynamical system, whose transfer functions are given by

$$G_{vm}(s) = \frac{J_{lr}s^2 + D_{el}s + K_{el}}{J_{lr}J_m s^3 + (JD_{el} + J_{lr}D_m)s^2 + (JK_{el} + D_m D_{el})s + D_m K_{el}}$$

$$G_{vl}(s) = \frac{D_{el}s + K_{el}}{J_{lr}J_m s^3 + (JD_{el} + J_{lr}D_m)s^2 + (JK_{el} + D_m D_{el})s + D_m K_{el}}$$

where $J_{lr} = J_l/n^2$ and $J = J_{lr} + J_m$.

Two-mass model of a servomechanism (III)

Assuming $D_m = 0$ and introducing the following parameters

$$\rho = \frac{J_{lr}}{J_m} \qquad \text{inertia ratio}$$

$$\omega_z = \sqrt{\frac{K_{el}}{J_{lr}}} \quad \xi_z = \frac{D_{el}}{2}\frac{1}{\sqrt{J_{lr}K_{el}}} \qquad \text{zero frequency and damping}$$

$$\omega_p = \omega_z\sqrt{1+\rho} \quad \xi_p = \xi_z\sqrt{1+\rho} \qquad \text{pole frequency and damping}$$

$$\mu = \frac{1}{J}$$

the two transfer functions become

$$G_{vm}(s) = \frac{\mu}{s}\frac{1+2\frac{\xi_z}{\omega_z}s+\frac{s^2}{\omega_z^2}}{1+2\frac{\xi_p}{\omega_p}s+\frac{s^2}{\omega_p^2}}$$

$$G_{vl}(s) = \frac{\mu}{s}\frac{1+2\frac{\xi_z}{\omega_z}s}{1+2\frac{\xi_p}{\omega_p}s+\frac{s^2}{\omega_p^2}}$$

rigid model

Two-mass model of a servomechanism (III)

Assuming $D_m = 0$ and introducing the following parameters

$$\rho = \frac{J_{lr}}{J_m} \qquad \text{inertia ratio}$$

$$\omega_z = \sqrt{\frac{K_{el}}{J_{lr}}} \quad \xi_z = \frac{D_{el}}{2}\frac{1}{\sqrt{J_{lr}K_{el}}} \qquad \text{zero frequency and damping}$$

$$\omega_p = \omega_z\sqrt{1+\rho} \quad \xi_p = \xi_z\sqrt{1+\rho} \qquad \text{pole frequency and damping}$$

$$\mu = \frac{1}{J}$$

the two transfer functions become

$$G_{vm}(s) = \frac{\mu}{s}\frac{1+2\frac{\xi_z}{\omega_z}s+\frac{s^2}{\omega_z^2}}{1+2\frac{\xi_p}{\omega_p}s+\frac{s^2}{\omega_p^2}}$$

$$G_{vl}(s) = \frac{\mu}{s}\frac{1+2\frac{\xi_z}{\omega_z}s}{1+2\frac{\xi_p}{\omega_p}s+\frac{s^2}{\omega_p^2}}$$

elastic behavior

Two-mass model of a servomechanism (IV)

Finally, in the case of no load torque, the system is represented by the following block diagram

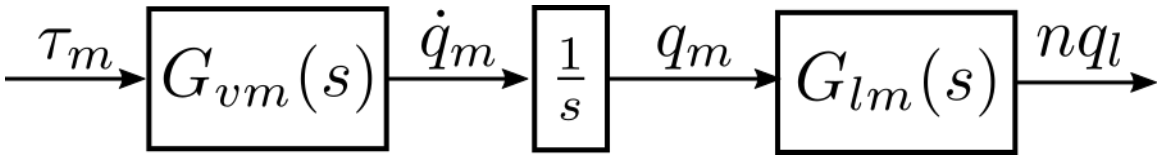

where

$$G_{lm}(s) = \frac{1 + 2\frac{\xi_z}{\omega_z}s}{1 + 2\frac{\xi_z}{\omega_z}s + \frac{s^2}{\omega_z^2}}$$

Two-mass model of a servomechanism (V)

The natural frequencies ω_p and ω_z have a clear physical interpretation.

ω_p, the system natural frequency, characterizes the zero-input response

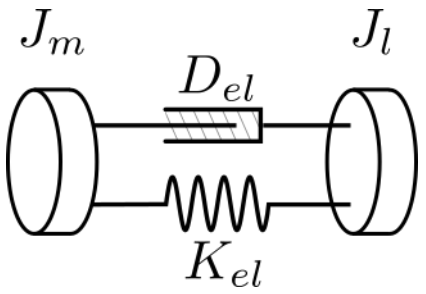

ω_z, the locked frequency, characterizes the oscillations of the load when the motor is locked

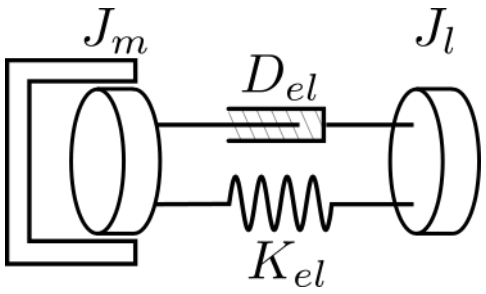

We will now analyze the transfer function $G_{vm}(s)$.

Two-mass model of a servomechanism (VI)

Consider again transfer function $G_{vm}(s)$

$$G_{vm}(s) = \frac{\mu}{s} \frac{1 + 2\frac{\xi_z}{\omega_z}s + \frac{s^2}{\omega_z^2}}{1 + 2\frac{\xi_p}{\omega_p}s + \frac{s^2}{\omega_p^2}}$$

Where are poles and zeros located in the complex plane?

We observe that

$$\frac{\omega_p}{\omega_z} = \frac{\xi_p}{\xi_z} = \sqrt{1+\rho} > 1$$

as a consequence

- poles' frequency is greater than zeros' frequency
- poles' damping is greater than zeros' damping

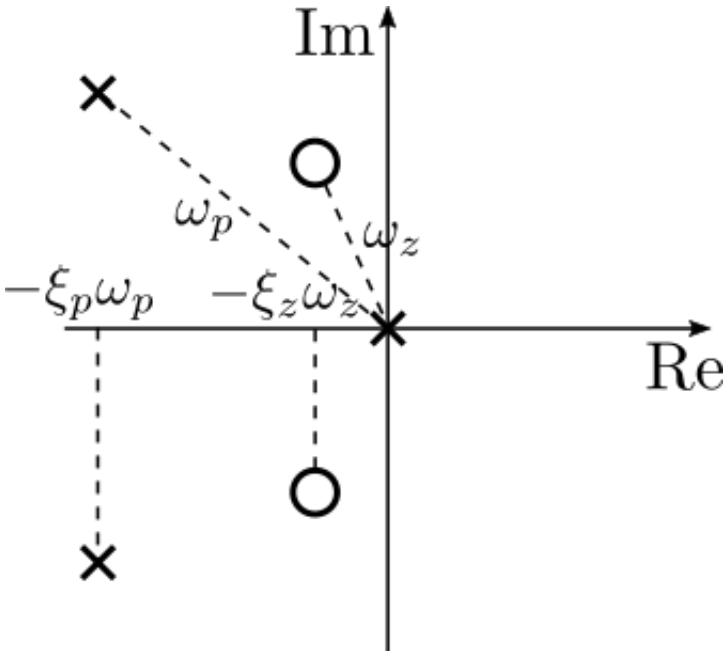

Two-mass model of a servomechanism (VII)

Consider again transfer function $G_{vm}(s)$

$$G_{vm}(s) = \frac{\mu}{s} \frac{1 + 2\frac{\xi_z}{\omega_z}s + \frac{s^2}{\omega_z^2}}{1 + 2\frac{\xi_p}{\omega_p}s + \frac{s^2}{\omega_p^2}}$$

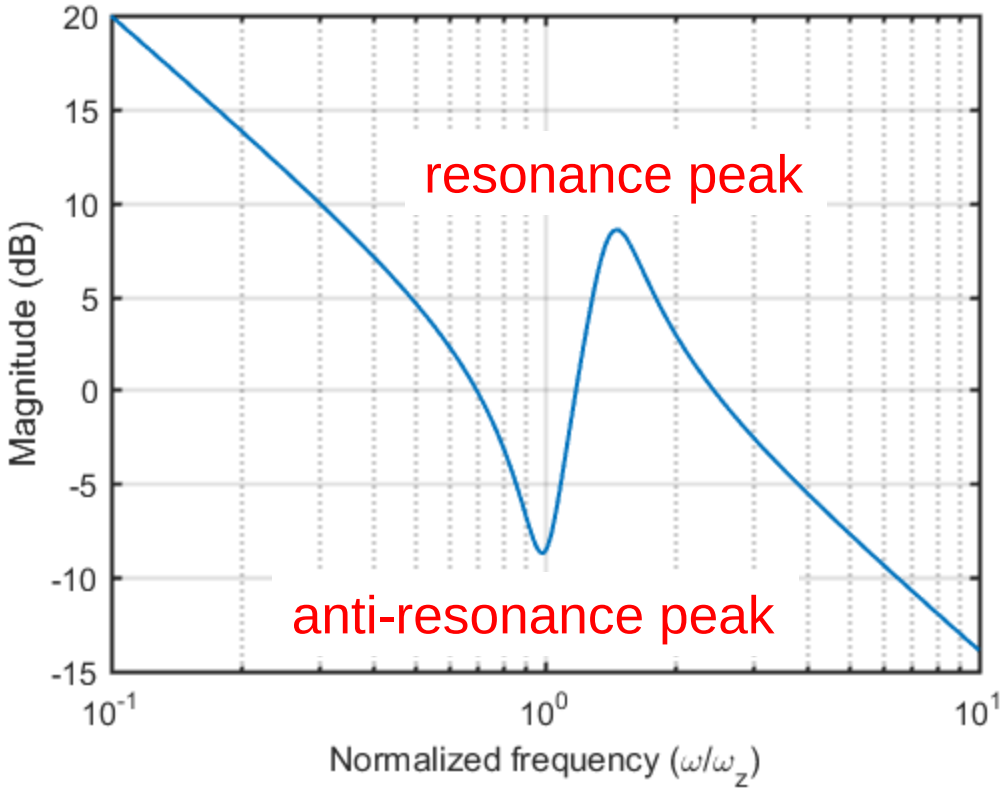

$\rho = 1 \quad \xi_z = 0.1$

Motor side P/PI control architecture

Introducing now the elastic model into the P/PI control scheme, assuming that only motor position/velocity measurements are available (as it usually happens in robotics) and neglecting load torque, we obtain

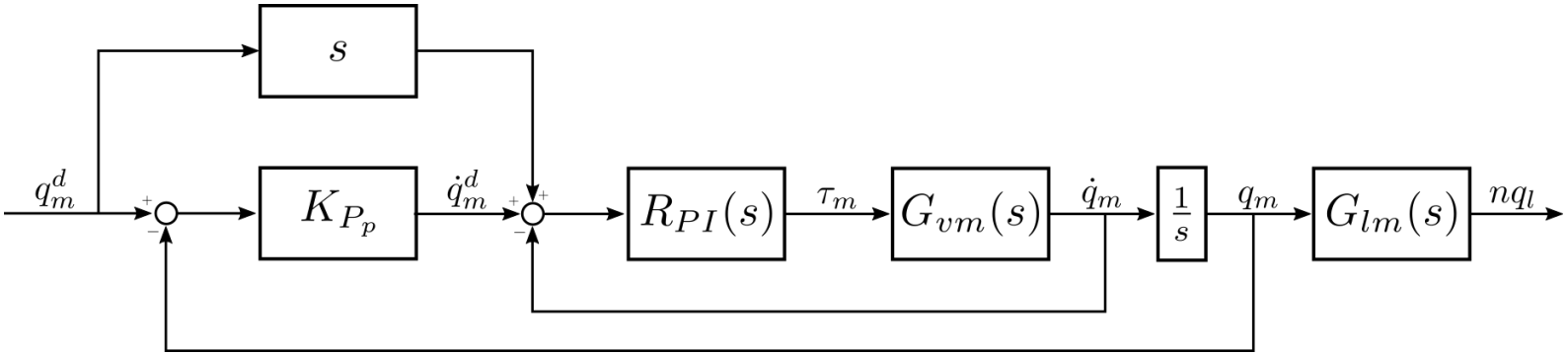

or, in case the velocity is computed elaborating the position measurement

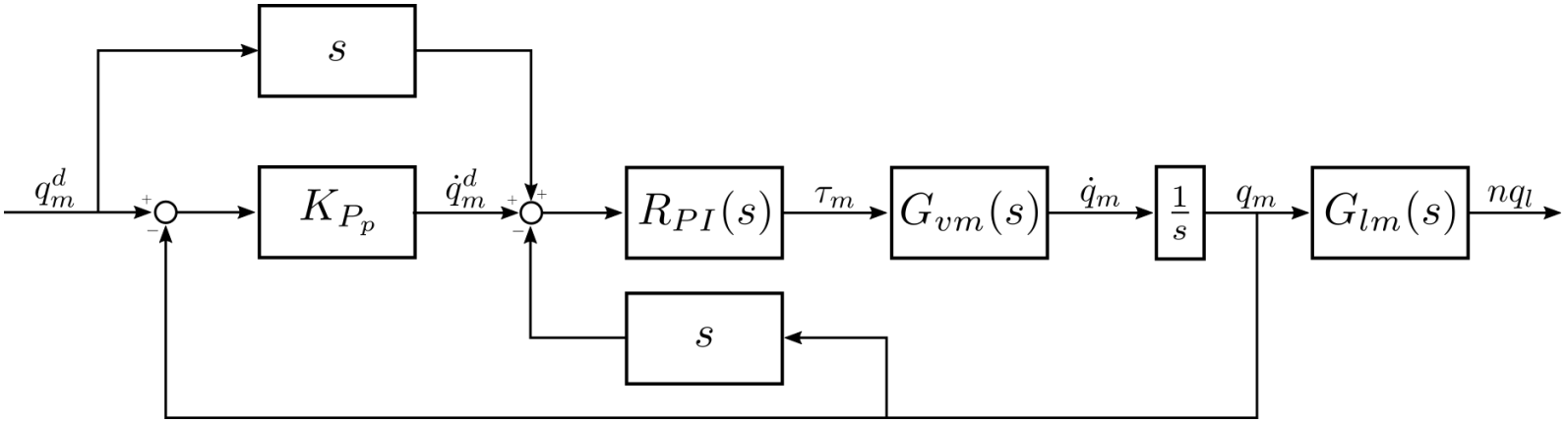

Velocity control (I)

Velocity control is accomplished using a PI controller

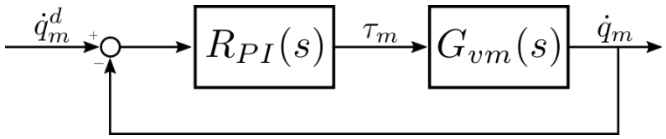

$$R_{PI}(s) = K_{P_v}\left(1 + \frac{1}{sT_{I_v}}\right) = K_{P_v}\frac{1 + sT_{Iv}}{sT_{Iv}}$$

The loop transfer function is given by

$$L_v(s) = R_{PI}(s)G_{vm}(s) = \frac{K_{P_v}\mu}{s}\frac{1 + sT_{I_v}}{sT_{I_v}}\frac{1 + 2\frac{\xi_z}{\omega_z}s + \frac{s^2}{\omega_z^2}}{1 + 2\frac{\xi_p}{\omega_p}s + \frac{s^2}{\omega_p^2}}$$

Let's introduce the following a-dimensional parameter

$$\tilde{\omega}_{c_v} = \frac{K_{P_v}\mu}{\omega_z}$$

that represents the crossover frequency computed using the rigid model and normalized with respect to the anti-resonance frequency.

The smaller $\tilde{\omega}_{c_v}$, the more cautious the project is.

Velocity control (II)

The integral time T_{I_v} can be selected in such a way that the controller zero is located one decade before the anti-resonance frequency

$$T_{I_v} = \frac{10}{\omega_z}$$

Let's look at the Bode plots we obtain with two different values of $\tilde{\omega}_{c_v}$.

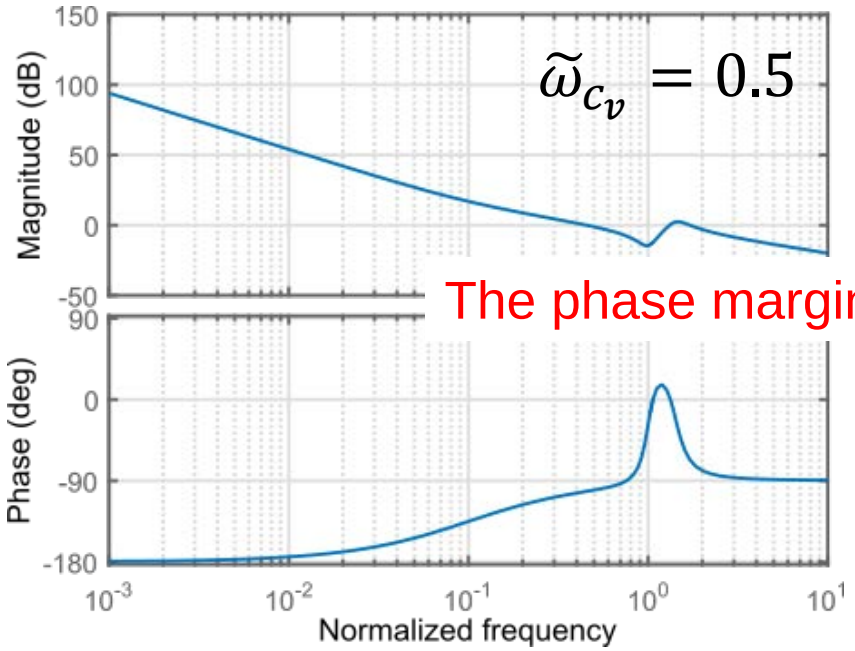

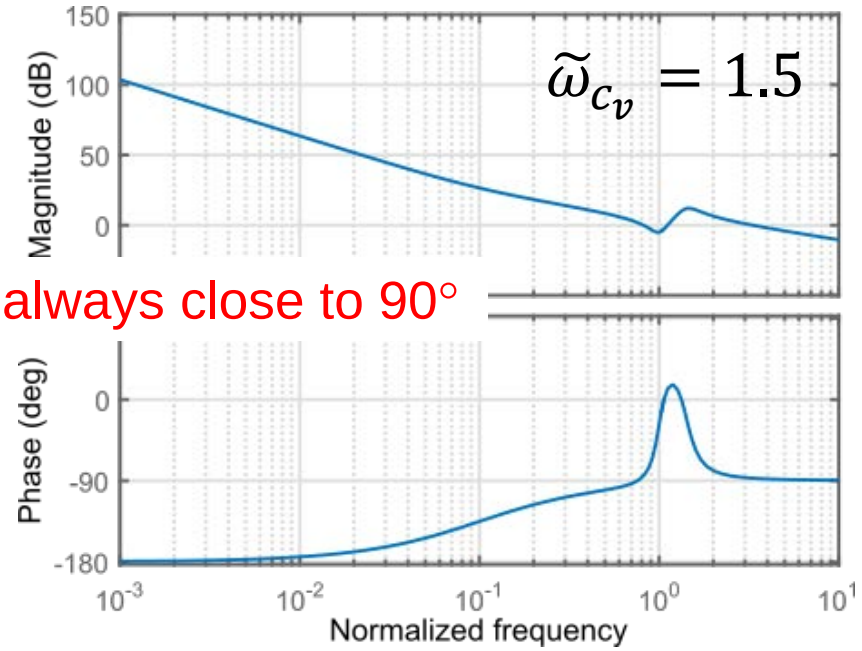

The phase margin is always close to 90°

$\rho = 1 \quad \xi_z = 0.1$

Velocity control (III)

From the previous result we conclude that both projects give rise to a closed-loop system that is robust asymptotically stable.

Let's try to analyze the Bode plot of the frequency response of the complementary sensitivity function with $\tilde{\omega}_{c_v} = 1.5$.

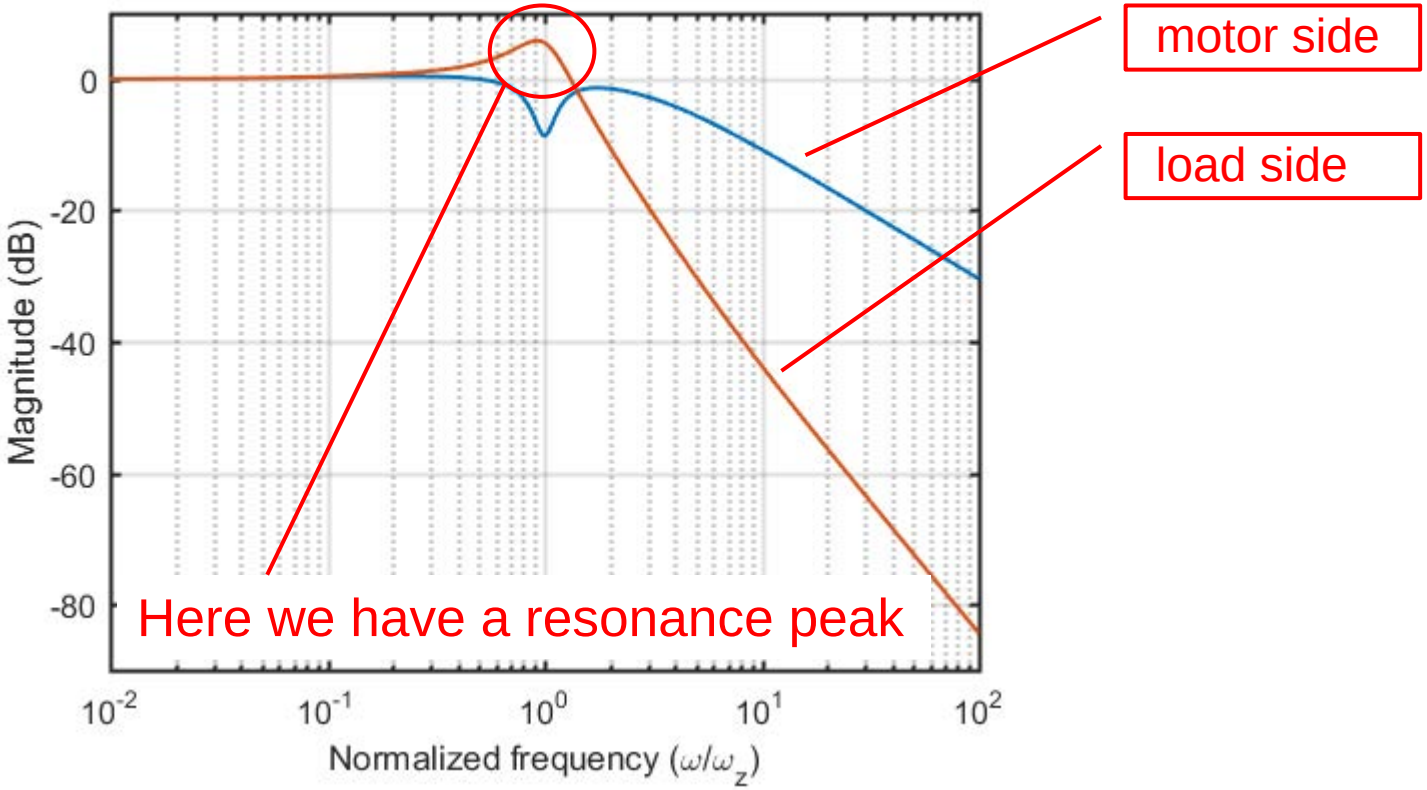

Velocity control (IV)

The clearest picture on the load oscillations is given by the root locus.

Let's consider the root locus with respect to $\tilde{\omega}_{c_v}$.

There are two complex poles whose damping is a function of $\tilde{\omega}_{c_v}$.

Maximum damping is achieved for

$$\tilde{\omega}_{c_v} \approx 0.7 \quad \Rightarrow \quad \omega_{c_v} \approx 0.7\omega_z$$

We will select as design rule

$$\tilde{\omega}_{c_v} \approx 0.7$$

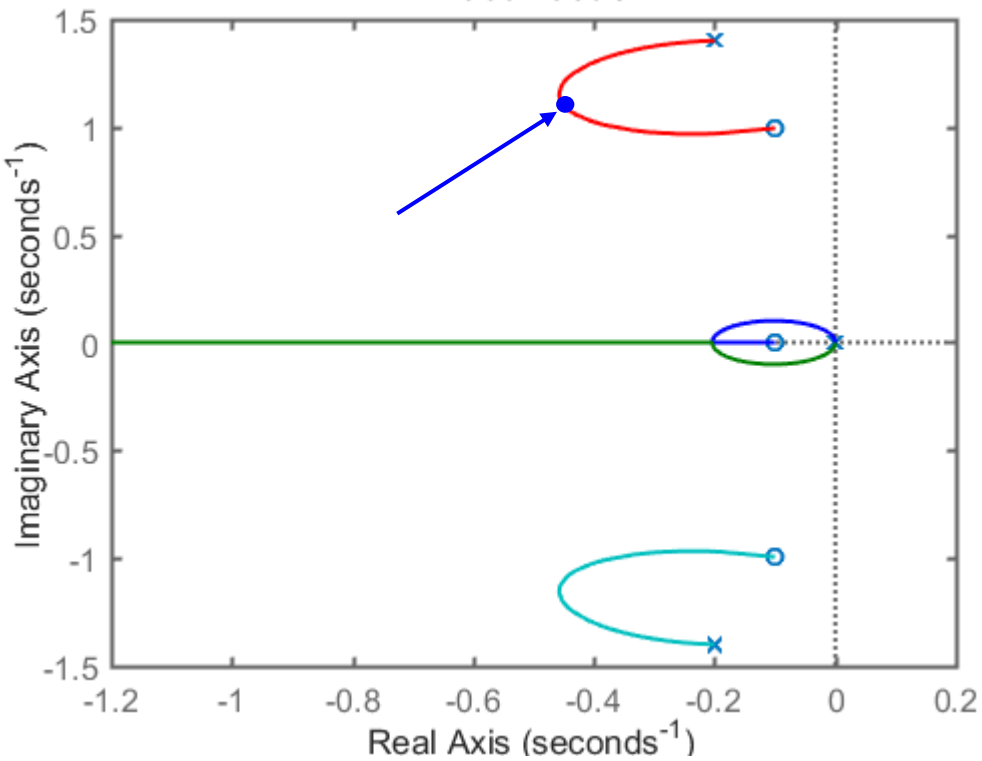

Root locus axis have been normalized with respect to ω_z.

Position control (I)

Position control is accomplished using a P controller.

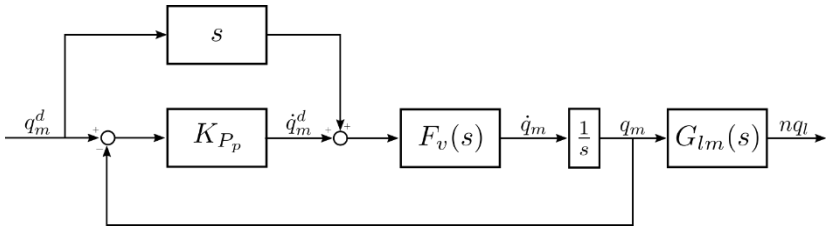

The loop transfer function is given by

$$L_p(s) = K_{P_p} \frac{F_v(s)}{s}$$

where

$$F_v(s) = \frac{L_v(s)}{1 + L_v(s)}$$

Let's introduce the following a-dimensional parameter

$$\tilde{\omega}_{c_p} = \frac{K_{P_p}}{\omega_z}$$

that represents the crossover frequency, computed using the rigid model, and normalized with respect to the anti-resonance frequency.

Position control (II)

Let's consider again the root locus of the loop transfer function

$$L_p(s) = K_{P_p} \frac{F_v(s)}{s} = \tilde{\omega}_{c_p} \frac{\omega_z}{s} F_v(s)$$

with respect to $\tilde{\omega}_{c_p}$ and for different values of $\tilde{\omega}_{c_v}$.

$\tilde{\omega}_{c_v} = 0.5$

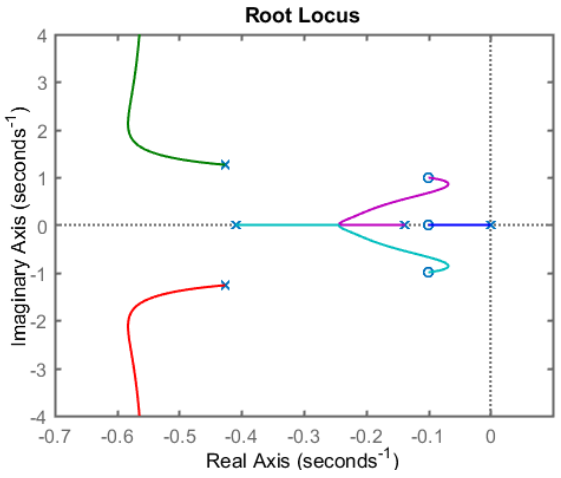

$\tilde{\omega}_{c_v} = 1$

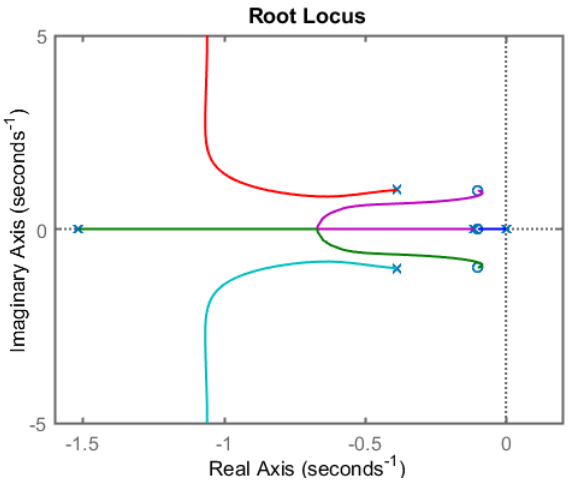

$\tilde{\omega}_{c_v} = 1.5$

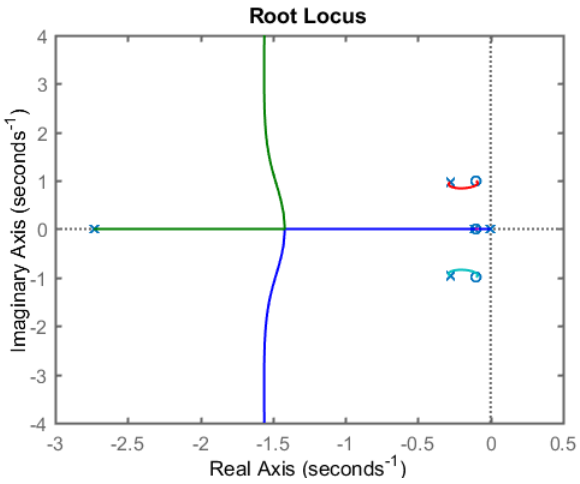

Increasing the bandwidth of the velocity loop, the damping of the closed-loop poles decreases.

Position control – Simulation example (I)

Let's see the results of the P/PI control on a simulation example.

The main characteristics of the servomechanism are

$$\omega_z = 200\ rad/s \quad \rho = 1 \quad \xi_z = 0.1$$

For the P/PI control

$$T_{I_v} = 10/\omega_z \quad \tilde{\omega}_{c_p} = 0.1$$

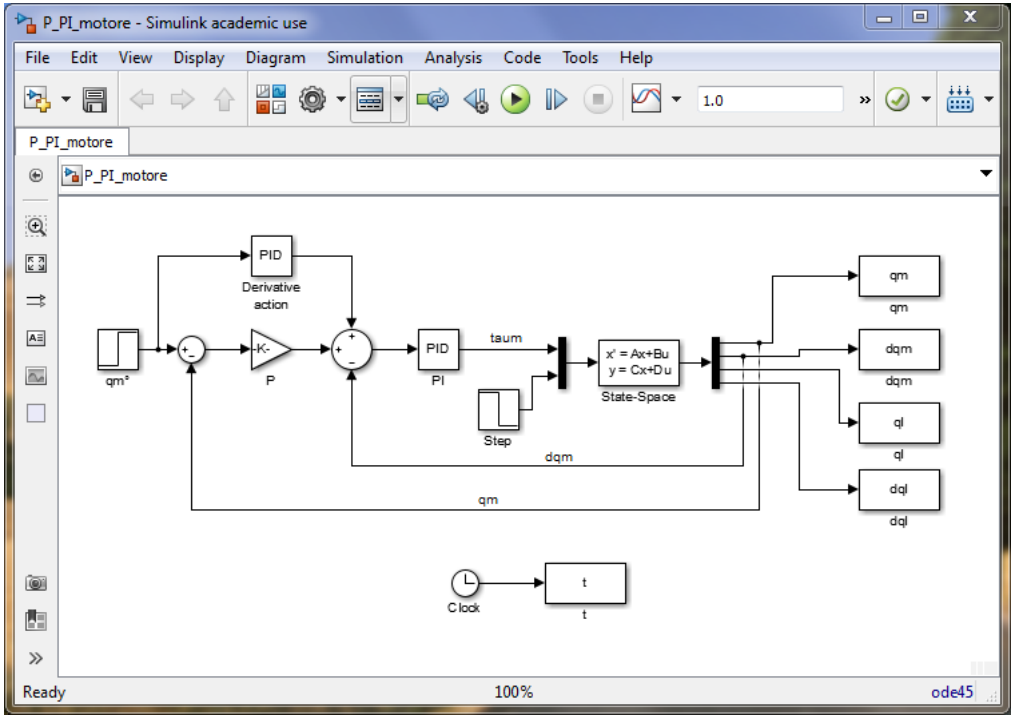

Position control – Simulation example (II)

$\tilde{\omega}_{c_v} = 0.5$

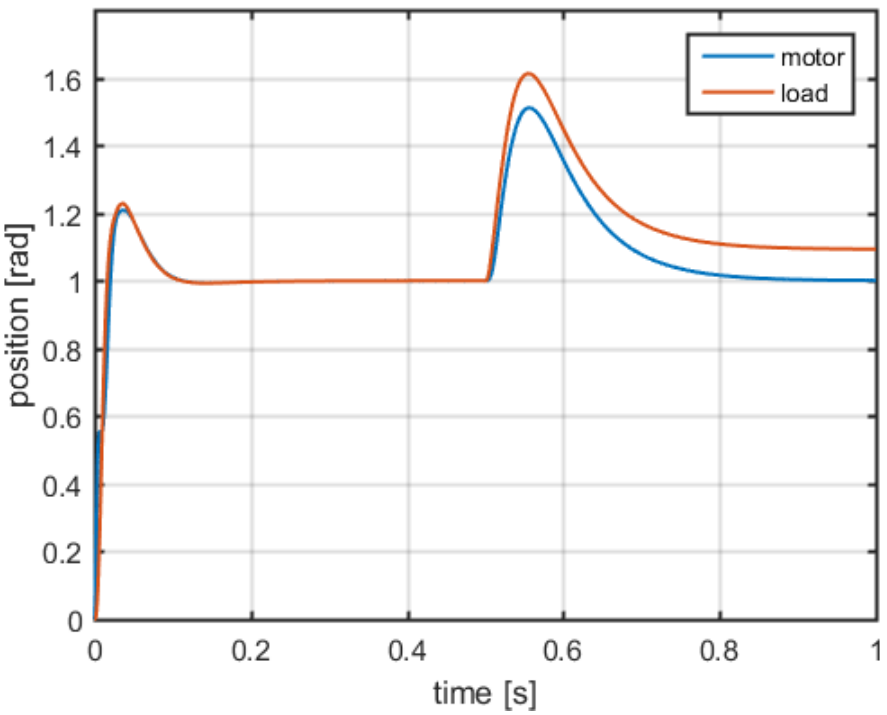

$\tilde{\omega}_{c_v} = 2.5$

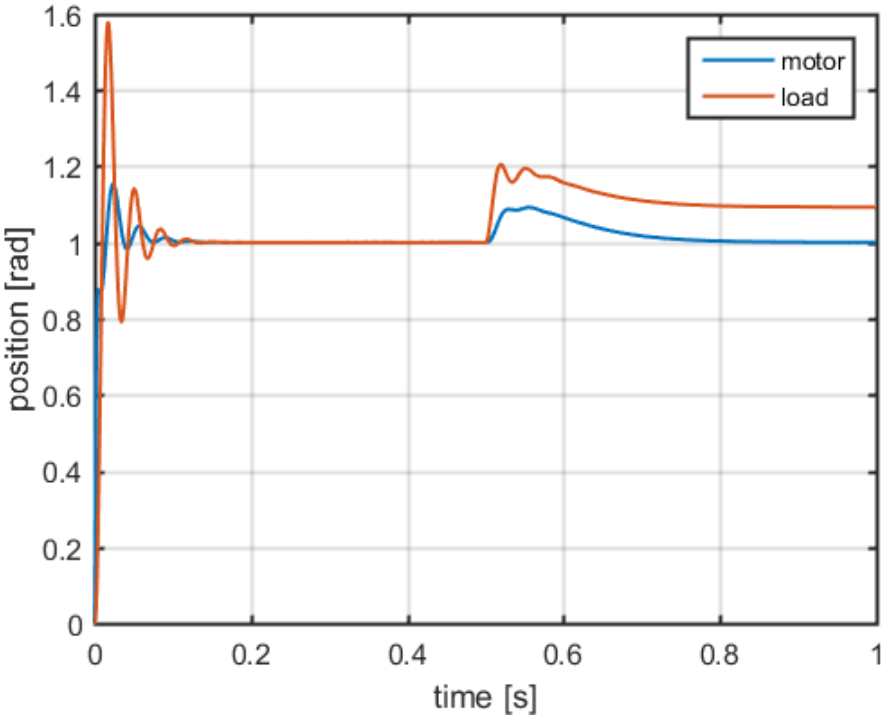

Motor side P/PI control performance limitations (I)

Root loci show that increasing the bandwidth of the velocity loop, performance of the motion control system referred to the load side decreases.

Can we quantify how much performance decreases?

Let's consider the transfer function from position set-point to load position

$$F_{lm}(s) = \frac{nq_l(s)}{q_m^d(s)}$$

$$\rho = 1 \quad \xi_z = 0.03$$
$$T_{I_v} = 10/\omega_z$$
$$\tilde{\omega}_{c_p} = 0.1$$

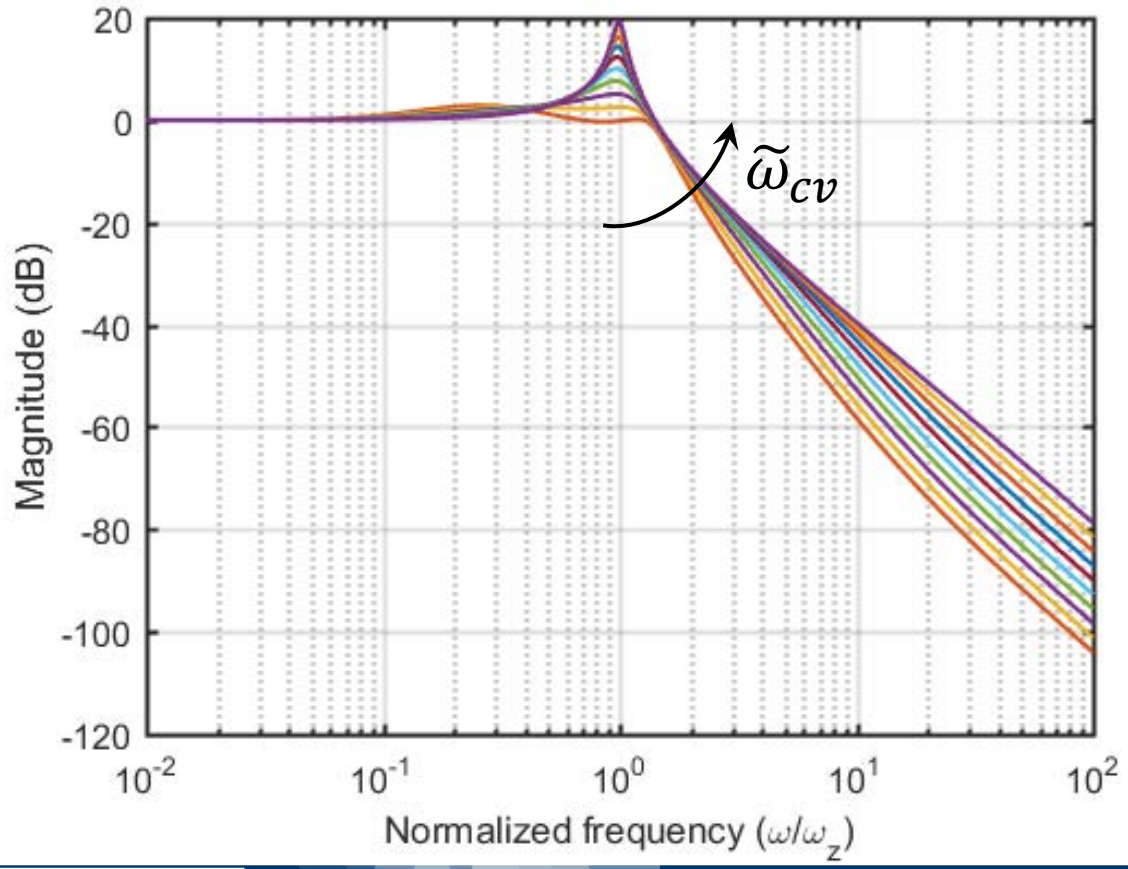

Motor side P/PI control performance limitations (II)

In order to characterize the performance limitations, we can study how the height of the resonance peak changes as a function of the velocity loop bandwidth.

This relation is given by the H_∞ norm of the transfer function

$$QL_\infty = \|F_{lm}(s)\|_\infty \approx \frac{1}{2\hat{\xi}} \qquad \hat{\xi} = \xi_z + \frac{1}{2\tilde{\omega}_{c_v}} \frac{\rho}{1+\rho}$$

and depends on

- servomechanism characteristics
- a design parameter of the velocity loop

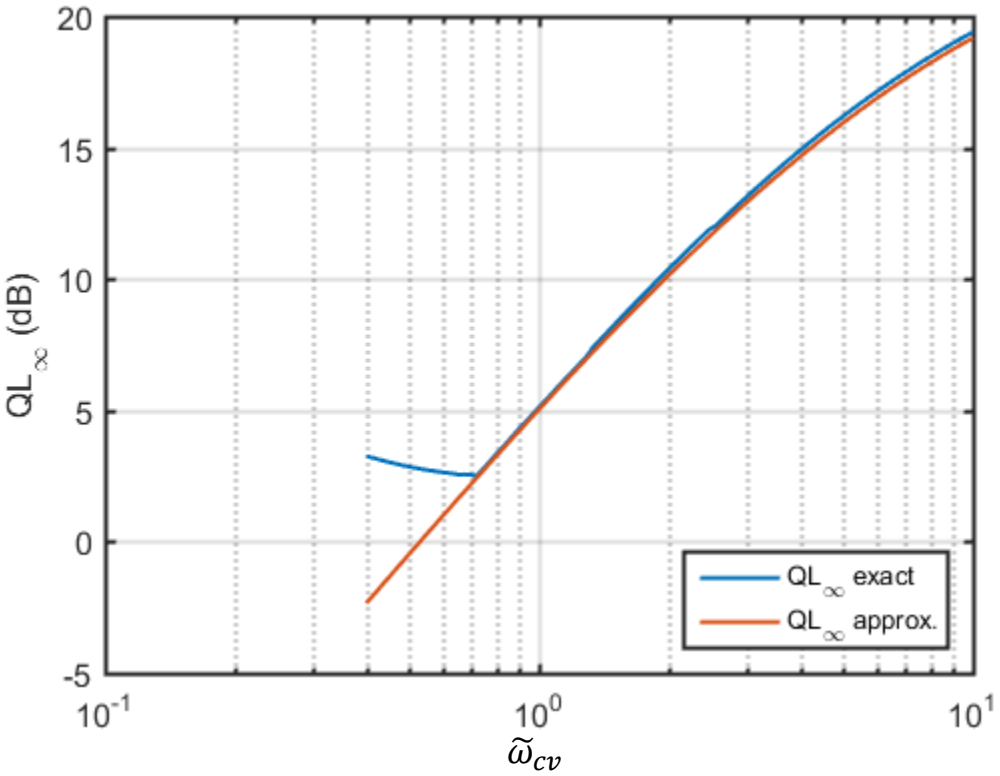

Load side P and motor side PI control architecture

In some applications, e.g., in machine tools, a load side (instead of a motor side) position control loop is adopted

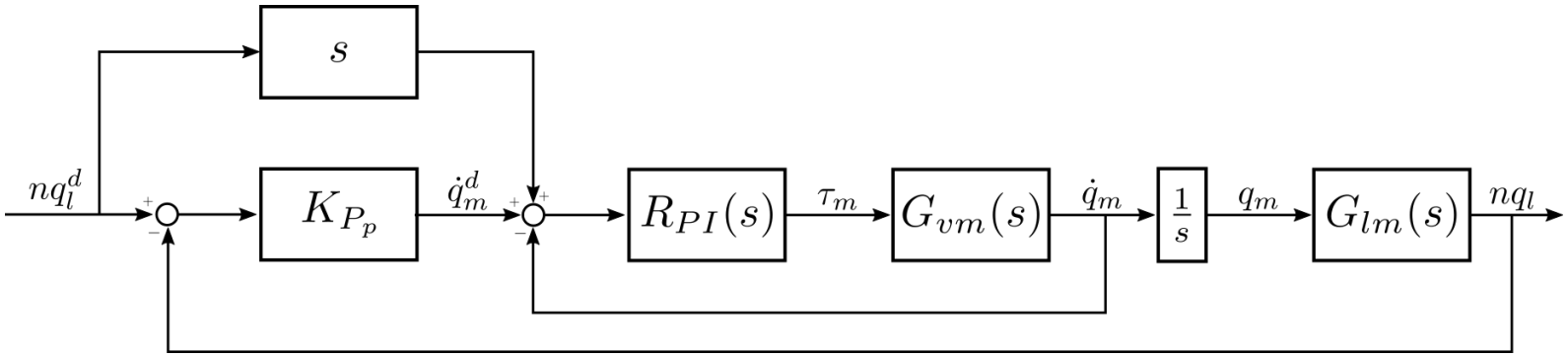

or, in case the velocity is computed elaborating the position measurement

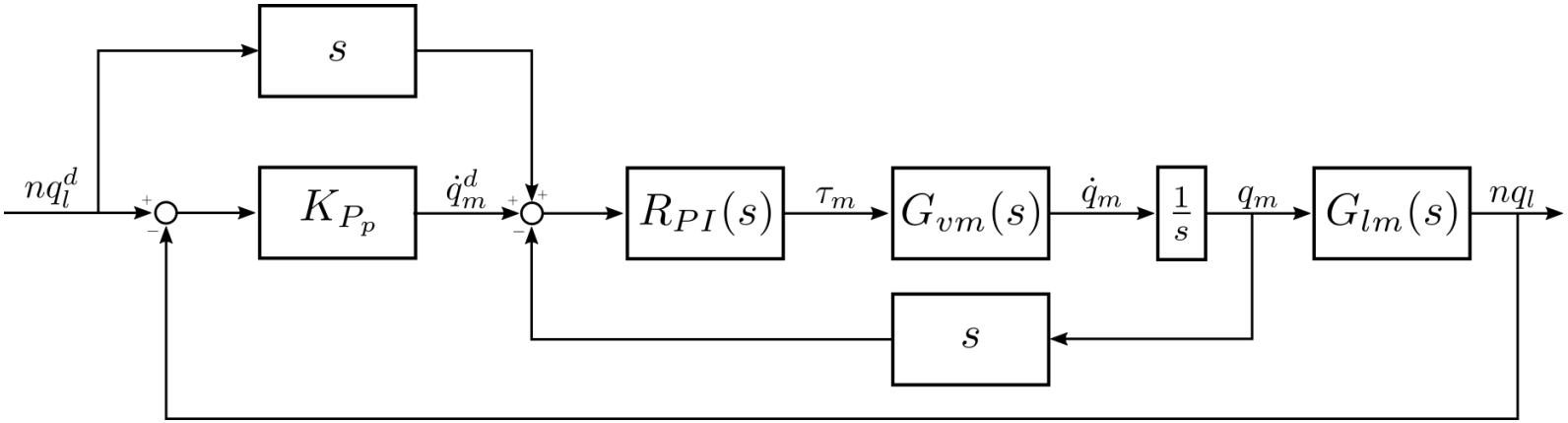

Position control (I)

Position control is still accomplished using a P controller.

The loop transfer function is given by

$$L_p(s) = K_{P_p} \frac{F_v(s)}{s} G_{lm}(s)$$

where

$$F_v(s) = \frac{L_v(s)}{1 + L_v(s)}$$

and

$$G_{lm}(s) = \frac{1 + 2\frac{\xi_z}{\omega_z} s}{1 + 2\frac{\xi_z}{\omega_z} s + \frac{s^2}{\omega_z^2}}$$

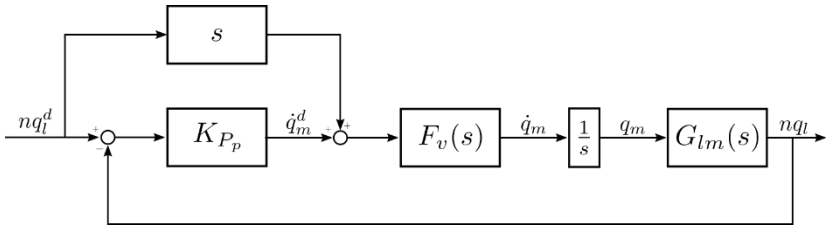

Position control (II)

Let's consider again the root locus of the loop transfer function

$$L_p(s) = K_{P_p} \frac{F_v(s)}{s} G_{lm}(s) = \tilde{\omega}_{c_p} \frac{\omega_z}{s} F_v(s) G_{lm}(s)$$

with respect to $\tilde{\omega}_{c_p}$ and for different values of $\tilde{\omega}_{c_v}$.

$\tilde{\omega}_{c_v} = 0.5$

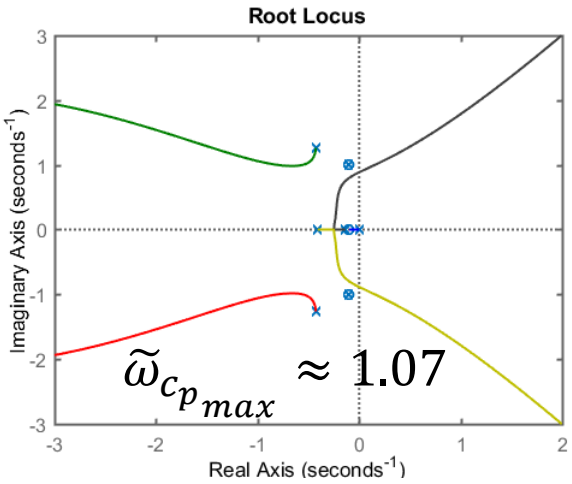

$\tilde{\omega}_{c_v} = 1$

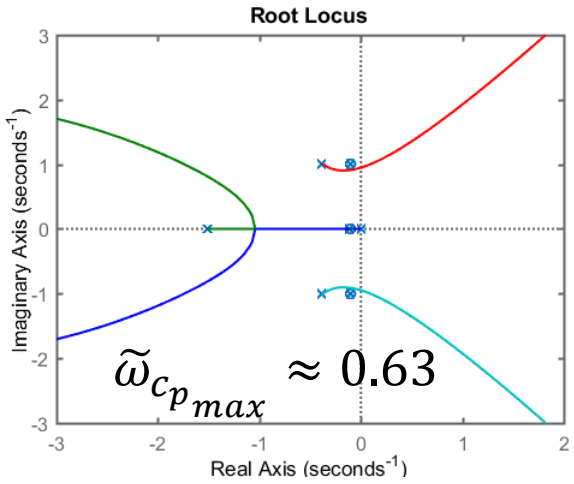

$\tilde{\omega}_{c_v} = 1.5$

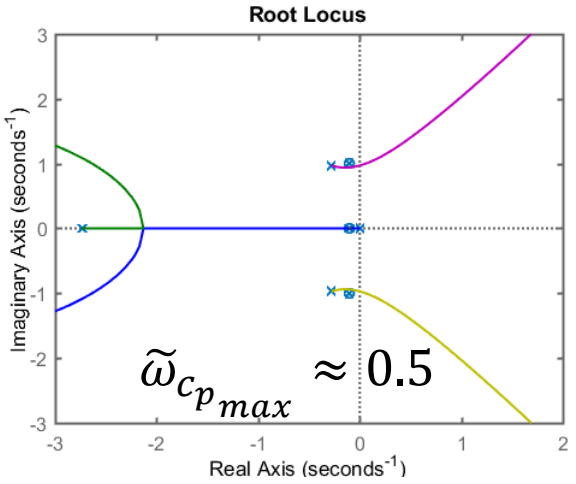

Increasing the bandwidth of the velocity loop, the design of the position loop becomes more and more complex (even small values of K_{P_p} can make the closed-loop system unstable).

Position control – Simulation example (I)

Let's see the results of the P/PI control on a simulation example.

The main characteristics of the servomechanism are

$$\omega_z = 200\ rad/s \quad \rho = 1 \quad \xi_z = 0.1$$

For the P/PI control

$$T_{I_v} = 10/\omega_z \quad \tilde{\omega}_{c_p} = 0.1$$

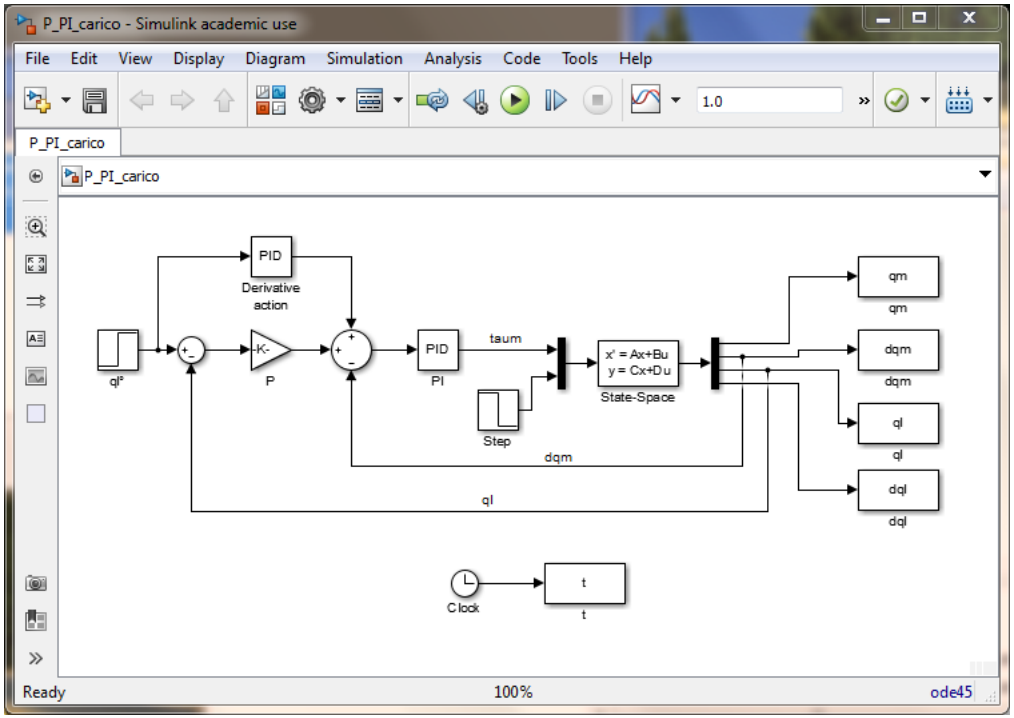

Position control – Simulation example (II)

$\tilde{\omega}_{c_v} = 0.5$

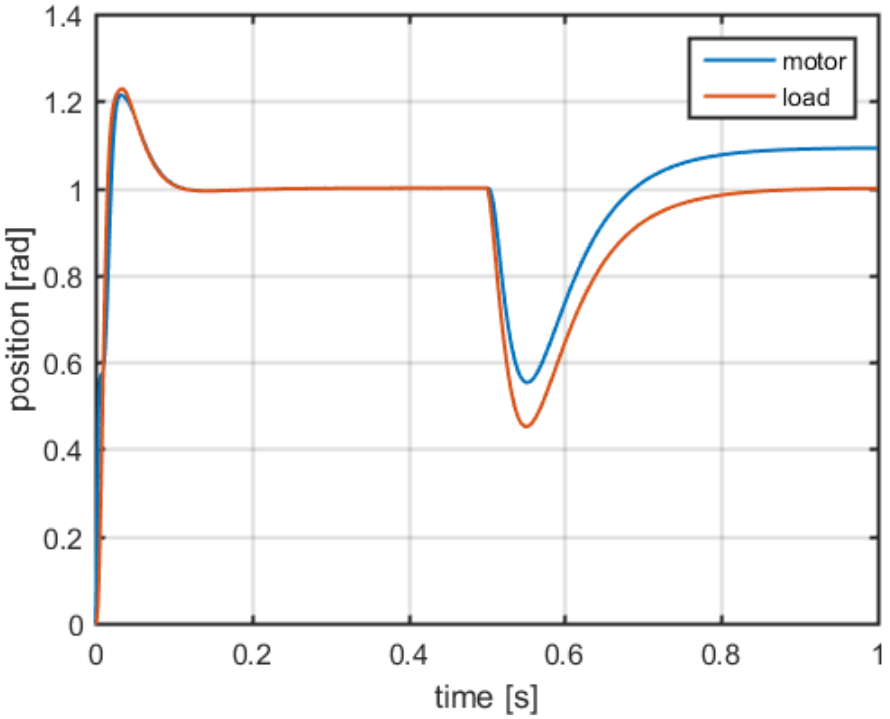

$\tilde{\omega}_{c_v} = 2.5$

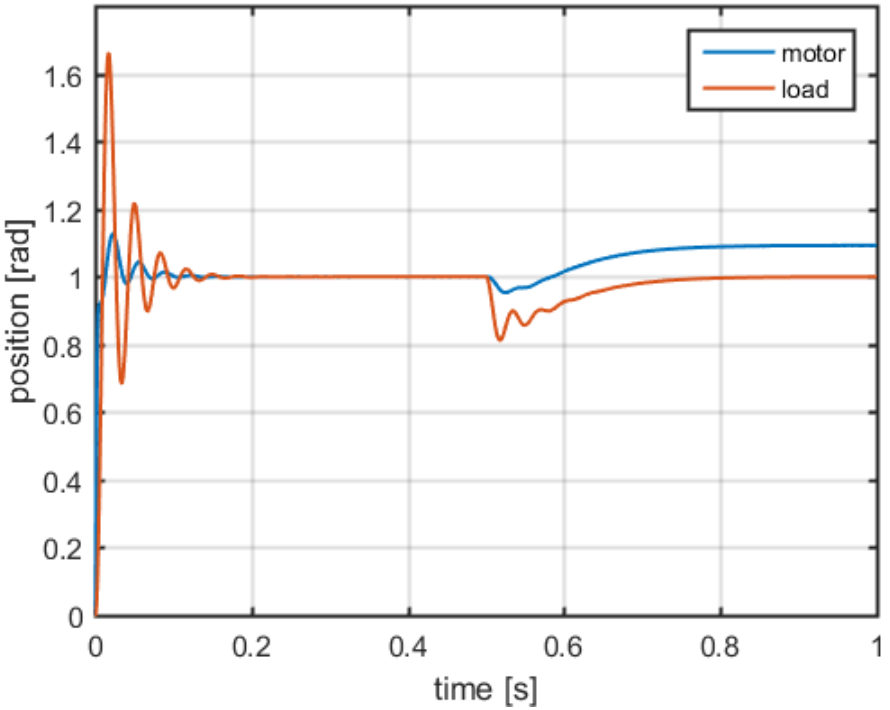

Position control – Simulation example (III)

Let's consider now $\tilde{\omega}_{c_p} = 0.7$ and $\tilde{\omega}_{c_v} = 1.5$.

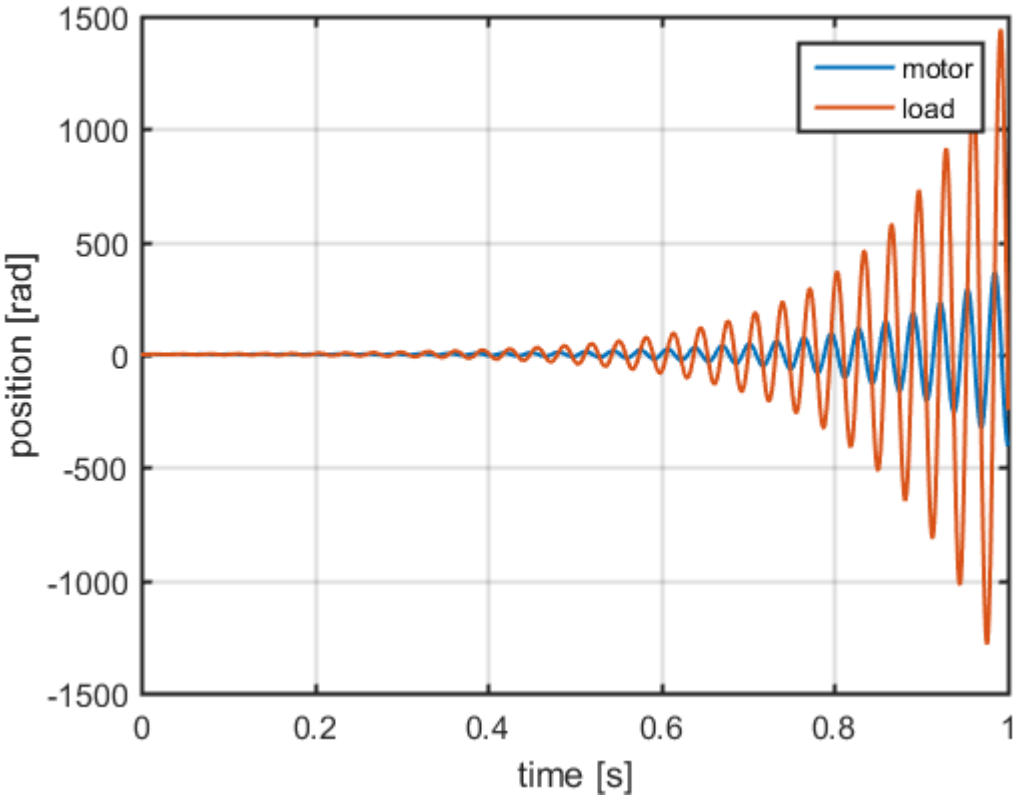

In this case the closed-loop system is unstable.

Load side P/PI control performance limitations (I)

Even in this case, root loci show that increasing the bandwidth of the velocity loop, performance of the motion control system referred to the load side decreases.

Let's consider the transfer function from position set-point to load position

$$F_{ll}(s) = \frac{nq_l(s)}{nq_l^d(s)}$$

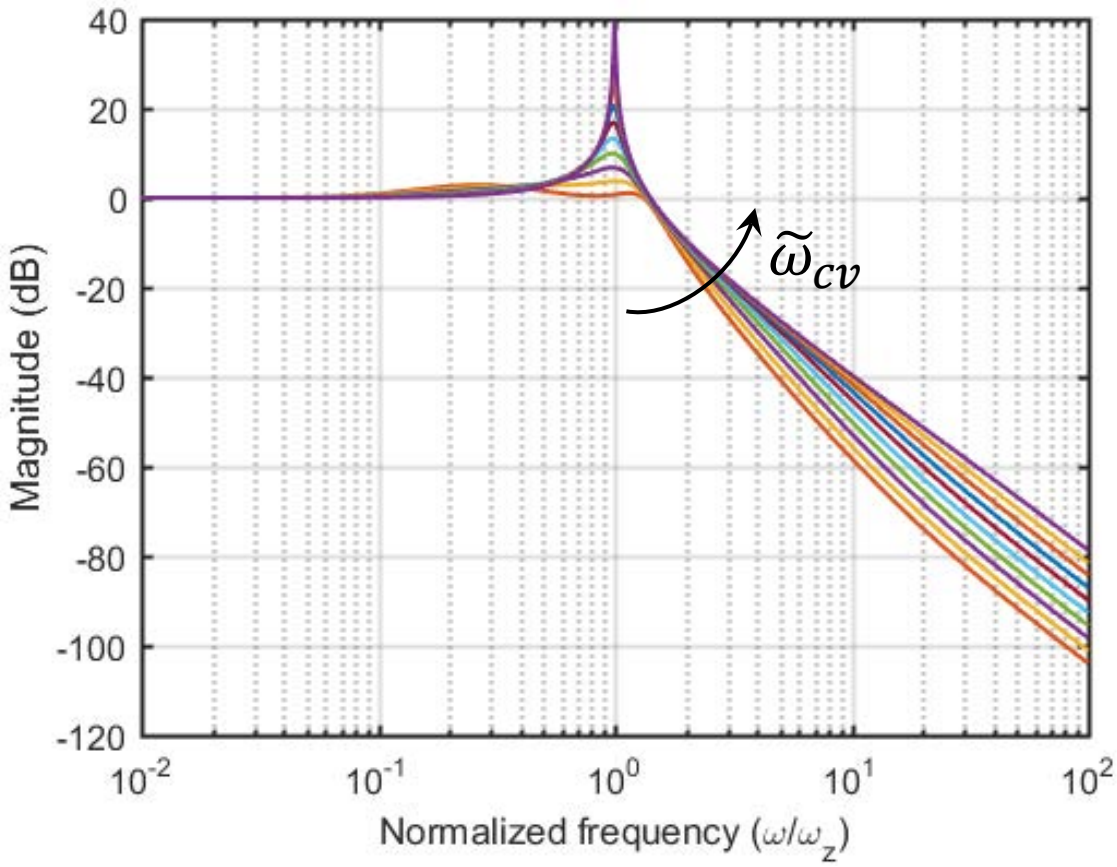

$$\rho = 1 \quad \xi_z = 0.03$$
$$T_{I_v} = 10/\omega_z$$
$$\tilde{\omega}_{c_p} = 0.1$$

Load side P/PI control performance limitations (II)

In order to characterize the performance limitations, we can study how the height of the resonance peak changes as a function of the velocity loop bandwidth.

This relation is given by the H_∞ norm of the transfer function

$$QL_\infty = \|F_{ll}(s)\|_\infty \approx \frac{1}{2\hat{\xi}} \qquad \hat{\xi} = \frac{\xi_z + \frac{1}{2\tilde{\omega}_{cv}}\frac{\rho}{1+\rho} - 0.5\tilde{\omega}_{cp}}{1 + \frac{\tilde{\omega}_{cp}}{\tilde{\omega}_{cv}}\frac{1}{1+\rho}}$$

Performance decrease is even more evident when a load side control architecture is considered.

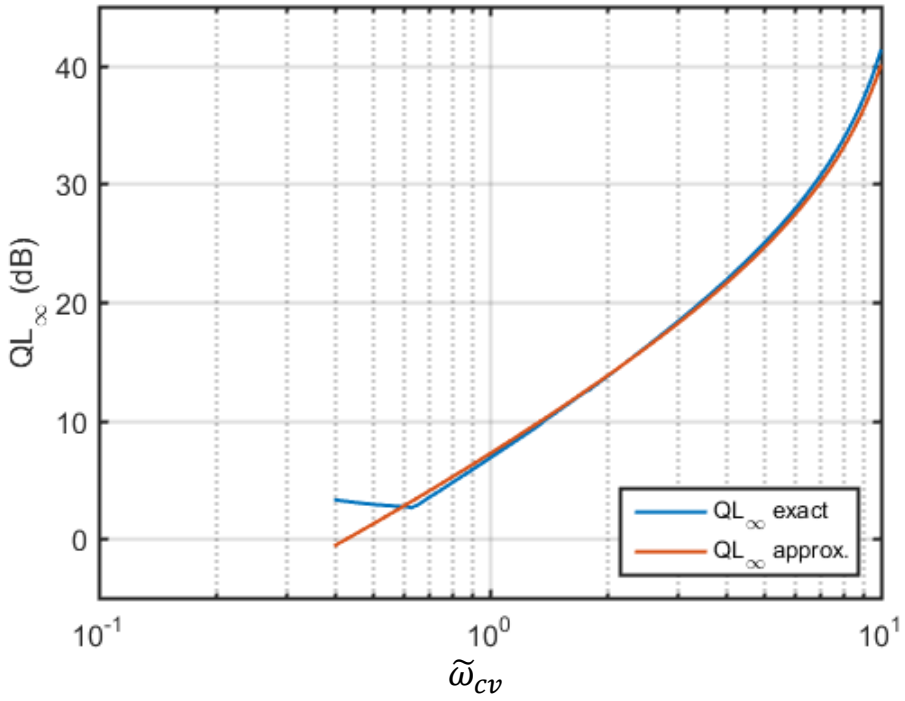

Servomechanism parameter identification (I)

To design the motion control system we need at least some of the parameters that describe its characteristics. In particular, we need an estimate of ξ_z, ω_z and ρ.

We will now introduce an algorithm to identify these parameters from experimental data.

First of all, consider that with a small bandwidth motion control system the closed-loop frequency response is very close to the open-loop one.

Furthermore, it can be shown that

$$r = \frac{|F_m(j\omega_p)|}{|F_m(j\omega_z)|} \approx \frac{1}{4\xi_z^2} \frac{\rho^2}{1+\rho^2}$$

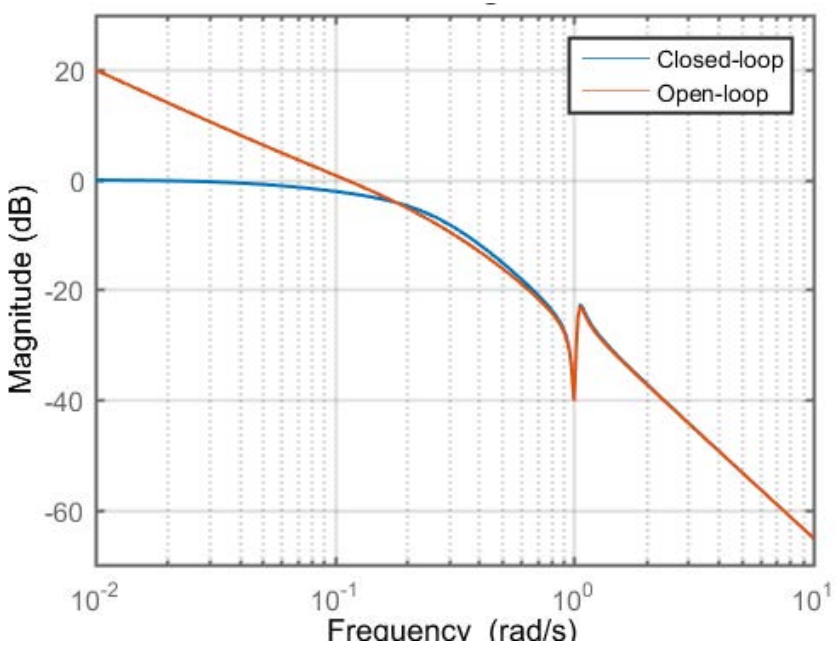

Servomechanism parameter identification (II)

We can thus adopt the following algorithm:

1. design a PID controller with $\omega_c \ll \hat{\omega}_z$, where $\hat{\omega}_z$ is a rough estimate of ω_z
2. execute an experiment (e.g., a sinusoidal chirp response) to get the graphical representation of $|F_m(j\omega)|$
3. from the plot one can compute ω_z, ω_p and
   $$r_{dB} = \left|F_m(j\omega_p)\right|_{dB} - \left|F_m(j\omega_z)\right|_{dB}$$
4. compute

$$r = 10^{\left(\frac{r_{dB}}{20}\right)}$$

$$\rho = \frac{\omega_p^2}{\omega_z^2} - 1$$

$$\xi_z = \frac{1}{2\sqrt{r}} \frac{\rho}{1+\rho}$$

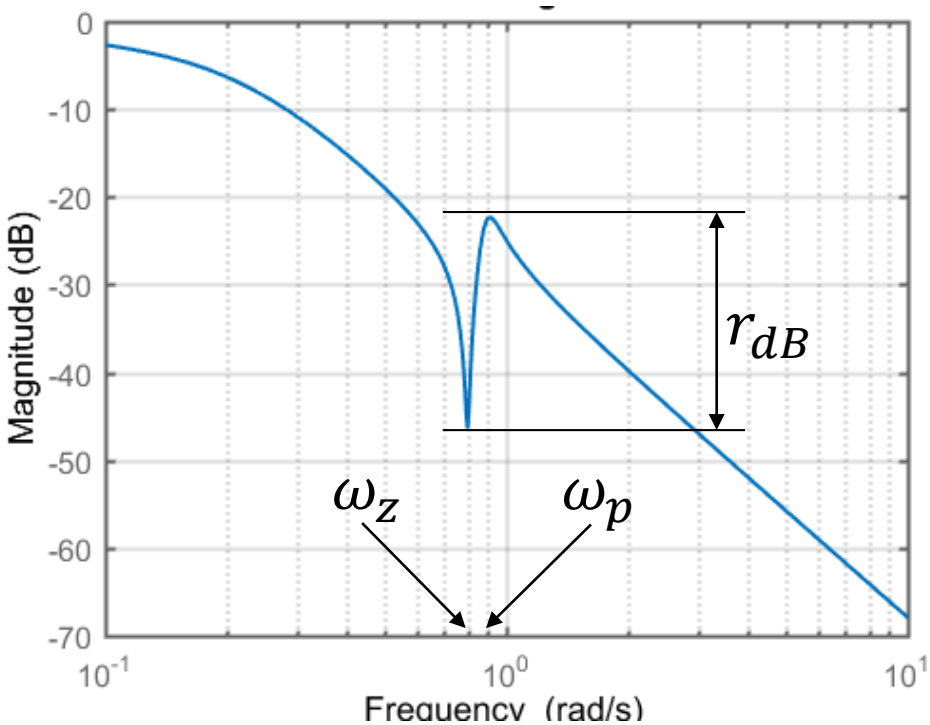

PID: derivative action and wind-up (I)

Motion control is accomplished using PID regulators.

We already saw that PID regulators are characterized by the following control law

$$u(t) = K_P e(t) + K_I \int_0^t e(\tau)\mathrm{d}\tau + K_D \frac{\mathrm{d}e(t)}{\mathrm{d}t}$$

or, in the frequency domain, by

$$R(s) = \frac{E(s)}{U(s)} = K_P \left(1 + \frac{1}{sT_I} + sT_D\right) = K_P \frac{T_I T_D s^2 + T_I s + 1}{sT_I}$$

This expression is very useful to design the regulator, as it characterizes its dynamical behavior. However, there are some problems, particularly important in applications, that are not evident from this simplified representation.

Two of these peculiar aspects are:

- realization of the derivative action
- regulator wind-up

PID: derivative action and wind-up (II)

The derivative action

$$u(t) = K_P T_D \frac{\mathrm{d}e(t)}{\mathrm{d}t} \qquad R_D(s) = K_P T_D s$$

corresponds to an a-causal system and cannot be realized in this form.

To make the derivative action realizable we introduce an high-frequency pole, that has also the effect of introducing a low-pass filtering action with respect to high frequency measurement noise.

The filtered derivative action has the following expression

$$R_D(s) = K_P \frac{sT_D}{1 + s\frac{T_D}{N}}$$

where N determines the frequency of the high frequency pole.

Increasing N the range of frequencies at which the derivative action acts as the ideal one increases, but the amplification applied to measurement noise increases as well.

N is usually selected in the range $5 - 10$.

PID: derivative action and wind-up (III)

Commercial PIDs differ from their academic counterpart not only for the expression of the derivative action.

Commercial regulators usually implement a standardized version of the PID control law, called PID standard ISA

$$U(s) = K_P \left(bY_{sp}(s) - Y(s) + \frac{1}{sT_I} E(s) + \frac{sT_D}{1 + sT_D/N} \left(cY_{sp}(s) - Y(s) \right) \right)$$

where Y_{sp} is the reference signal, b and c are two parameters that allow to weight in a different way the reference signal and the measurement in the proportional and derivative actions.

A PID standard ISA is a two-degree-of-freedom regulator: we can define two different transfer functions, one from the reference signal to the control signal, the other one from the measurement signal to the control signal.

PID: derivative action and wind-up (IV)

The transfer functions of the feedforward and feedback blocks are

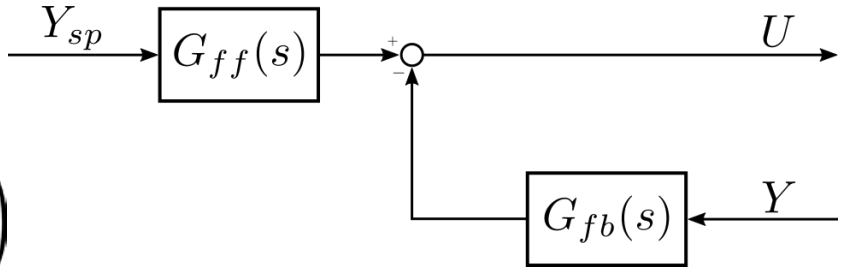

$$G_{ff}(s) = K_P\left(b + \frac{1}{sT_I} + c\frac{sT_D}{1+sT_D/N}\right)$$

$$G_{fb}(s) = K_P\left(1 + \frac{1}{sT_I} + \frac{sT_D}{1+sT_D/N}\right)$$

Using b and c one can select the zeros of the transfer function from set-point to controlled variable independently of the feedback part of the controller.

Considering, for example, a plant whose transfer function is

$$G(s) = \frac{1}{s^2}$$

we obtain

$$\frac{Y(s)}{Y_{sp}(s)} = G_{ff}(s)\frac{G(s)}{1+G(s)G_{fb}(s)} = \frac{cs^2T_DT_I + bsT_I + 1}{s^3\frac{T_I}{\mu K_P} + s^2T_DT_I + sT_I + 1}$$

PID: derivative action and wind-up (V)

Another problem that usually happens in applications is wind-up.

Any actuator is characterized by a maximum and minimum value of the physical variable on which it operates. We will represent this aspect introducing a symmetric saturation in the block diagram of the closed-loop system.

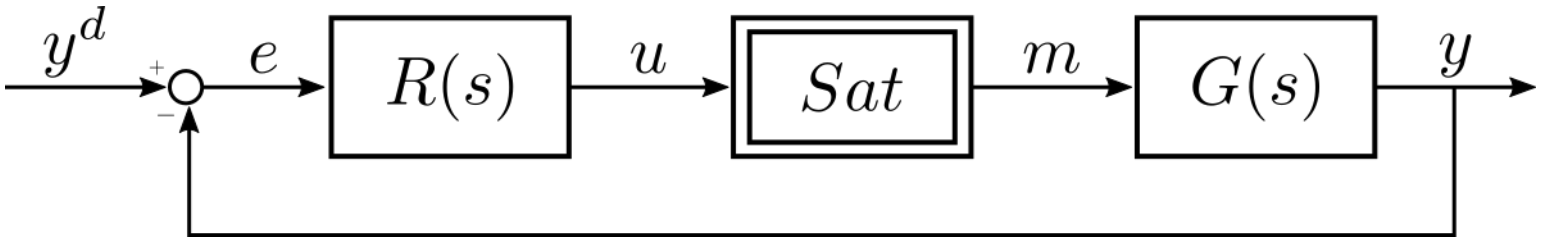

The saturation block is described by the following relation

$$m = \text{sign}(u)\,\min\left(\text{abs}(u), u_M\right)$$

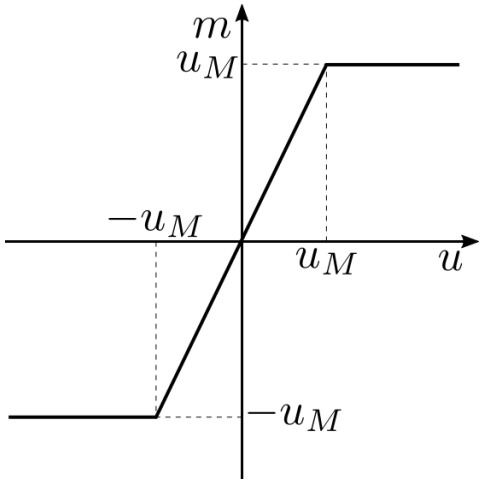

If the regulator as an integral action the saturation can generate an effect called integral wind-up, that causes a decrease in control performance.

PID: derivative action and wind-up (VI)

Let's consider a PID with only the integral action (I regulator), and assume that the error e keeps the same sign (e.g., positive) for a long time.

Consider the following sequence of events:

- the state of the integrator (and, consequently, the output of the regulator) indefinitely increases exceeding the saturation value u_M
- as a consequence the actuator saturates, i.e., $m = u_M$
- sooner or later y exceeds the reference value y^d, making the error e negative
- m should now take values less than u_M
- to achieve this desired behavior, however, one should wait that the high value of the integrator state (wind-up), and thus the output u, decreases below u_M

The time required to the integrator state to take values less than u_M can be rather long and, during this interval, there is a significant decay of control performance.

PID: derivative action and wind-up (VII)

A first solution to overcome the integral wind-up is by changing the regulator implementation.

Consider, for example, a PI regulator

$$R(s) = K_P \left(1 + \frac{1}{sT_I}\right)$$

we could implement it in the following anti-windup configuration

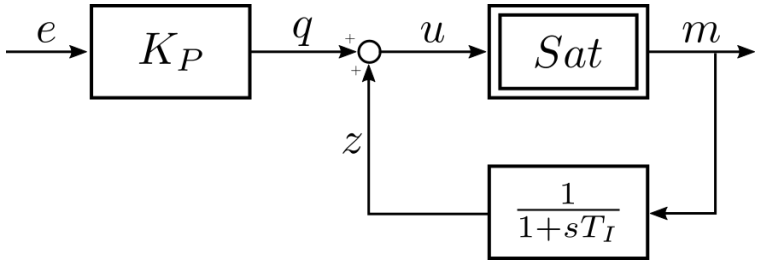

When the saturation is not active, the saturation block is equivalent to a unitary gain and the regulator transfer function becomes

$$R(s) = K_P \frac{1}{1 - \frac{1}{1+sT_I}} = K_P \left(1 + \frac{1}{sT_I}\right)$$

PID: derivative action and wind-up (VIII)

Consider again the following sequence of events:

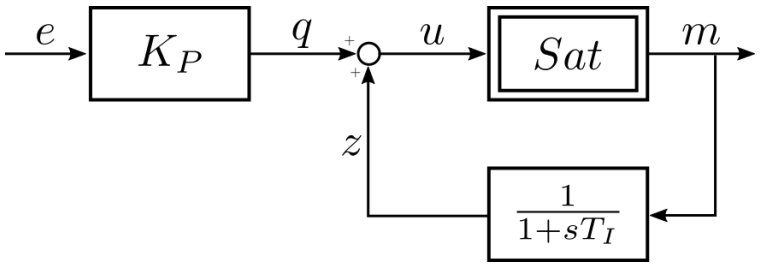

- the error e keeps the same sign (e.g., positive) for a long time
- assuming $K_P > 0$, then $q > 0$
- assume that the actuator saturates, i.e., $m = u_M$
- as the feedback block is a unitary gain transfer function, the steady-state value of z is u_M
- sooner or later y exceeds the reference value y^d, making the error e negative
- when the sign of the error changes, the sign of q changes as well and, as $z = u_M$, u takes values less than u_M (the actuator does not saturate anymore)

PID: derivative action and wind-up (IX)

Another solution to the integral wind-up is by stopping the computation of the integral action when the actuator saturates (conditional integration).